Acta Pharmaceutica Sinica B 2025;15(2):1039−1055

Chinese Pharmaceutical Association
Institute of Materia Medica, Chinese Academy of Medical Sciences

Acta Pharmaceutica Sinica B

www.elsevier.com/locate/apsb
www.sciencedirect.com


ORIGINAL ARTICLE

# Deubiquitinase JOSD2 alleviates colitis by inhibiting inflammation *via* deubiquitination of IMPDH2 in macrophages

**Xin Liu[a,b,c,†], Yi Fang[c,†], Mincong Huang[d], Shiliang Tu[b], Boan Zheng[b], Hang Yuan[b], Peng Yu[b], Mengyao Lan[d], Wu Luo[c], Yongqiang Zhou[e], Guorong Chen[f], Zhe Shen[g], Yi Wang[c], Guang Liang[a,c,d,*]**

[a]*Department of Pharmacy and Institute of Inflammation, Zhejiang Provincial People's Hospital, Affiliated People's Hospital of Hangzhou Medical College, Hangzhou 310014, China*
[b]*Department of Colorectal Surgery, Zhejiang Provincial People's Hospital, Affiliated People's Hospital of Hangzhou Medical College, Hangzhou 310014, China*
[c]*Chemical Biology Research Center, School of Pharmaceutical Sciences, Wenzhou Medical University, Wenzhou 325035, China*
[d]*Zhejiang TCM Key Laboratory of Pharmacology and Translational Research of Natural Products, School of Pharmaceutical Sciences, Hangzhou Medical College, Hangzhou 311399, China*
[e]*Department of Radiation and Medical Oncology, the First Affiliated Hospital of Wenzhou Medical University, Wenzhou 325035, China*
[f]*Department of Pathology, the Affiliated Quzhou Hospital of Wenzhou Medical University, Quzhou 32400, China*
[g]*The Department of Gastroenterology, the First Affiliated Hospital, School of Medicine, Zhejiang University, Hangzhou 310003, China*

Received 1 June 2024; received in revised form 17 July 2024; accepted 22 October 2024

**KEY WORDS**

Colitis;
Deubiquitinase;
JOSD2;
IMPDH2;

**Abstract** Inflammatory bowel disease (IBD) is a chronic inflammatory disorder of the gastrointestinal tract, which increases the incidence of colorectal cancer (CRC). In the pathophysiology of IBD, ubiquitination/deubiquitination plays a critical regulatory function. Josephin domain containing 2 (JOSD2), a deubiquitinating enzyme, controls cell proliferation and carcinogenesis. However, its role in IBD remains unknown. Colitis mice model developed by dextran sodium sulfate (DSS) or colon tissues from

*Corresponding author.
E-mail address: wzmcliangguang@163.com (Guang Liang).
[†]These authors made equal contributions to this work.
Peer review under the responsibility of Chinese Pharmaceutical Association and Institute of Materia Medica, Chinese Academy of Medical Sciences.

https://doi.org/10.1016/j.apsb.2024.12.012

Inflammation;
Inflammatory bowel disease;
Macrophage;
Nuclear factor kappa B

individuals with ulcerative colitis and Crohn's disease showed a significant upregulation of JOSD2 expression in the macrophages. JOSD2 deficiency exacerbated the phenotypes of DSS-induced colitis by enhancing colon inflammation. DSS-challenged mice with myeloid-specific JOSD2 deletion developed severe colitis after bone marrow transplantation. Mechanistically, JOSD2 binds to the C-terminal of inosine-5′-monophosphate dehydrogenase 2 (IMPDH2) and preferentially cleaves K63-linked polyubiquitin chains at the K134 site, suppressing IMPDH2 activity and preventing activation of nuclear factor kappa B (NF-κB) and inflammation in macrophages. It was also shown that JOSD2 knockout significantly exacerbated increased azoxymethane (AOM)/DSS-induced CRC, and AAV6-mediated JOSD2 overexpression in macrophages prevented the development of colitis in mice. These outcomes reveal a novel role for JOSD2 in colitis through deubiquitinating IMPDH2, suggesting that targeting JOSD2 is a potential strategy for treating IBD.



## 1. Introduction

Inflammatory bowel disease (IBD), encompassing Crohn's disease (CD) and ulcerative colitis (UC), is a recurring, heterogeneous, and chronically affecting inflammatory illness of the gastrointestinal tract. The development of this condition is primarily influenced by an intricate combination of genetic susceptibility and environmental influence that disrupts the interactions between the host and the microbiota, leading to an imbalance in the immunological responses of the gut. Furthermore, individuals with IBD have a heightened susceptibility to acquiring colorectal cancer (CRC) that is associated with colitis[1,2]. As a result of its ability to initiate and promote carcinogenesis, IBD has been identified as a high-risk disease condition associated with CRC[3]. Recent studies have revealed that, during IBD, innate immune cells like neutrophils and macrophages invade the gut and release inflammatory cytokines[4,5]. The subsequent deterioration of intestinal epithelial cells and compromise of intestinal homeostasis result from increased inflammation[6,7]. However, the detailed mechanisms underlying inflammatory regulation in macrophages involved in IBD remain elusive. Thus, understanding the pathophysiology of IBD and developing novel treatment options for IBD and CRC requires the identification of the specific processes related to regulation that governs immunological and inflammatory responses in the gut.

The occurrence and progression of IBD are known to be associated with many regulatory mechanisms[8,9]. Ubiquitination and deubiquitination, which are post-translational modifications of proteins, have recently been demonstrated to control the homeostasis and dysfunction of the intestines[10]. One common protein modification that happens in a variety of ways throughout various biological activities is ubiquitination[11]. It is frequently observed at lysine residues, such as Lys63, Lys48, Lys33, Lys29, Lys27, Lys11, and Lys6, of substrate proteins and ubiquitin[12]. E3 ubiquitin ligases are primarily responsible for the substrate selectivity of ubiquitination. Two reversible mechanisms include deubiquitinase (DUB)-mediated deubiquitination and E3-mediated ubiquitination. It has been observed that DUBs target crucial proteins implicated in colonic inflammatory signaling pathways through deubiquitinating regulators[13]. For example, in intestinal epithelial cells, the K63-linked polyubiquitination of tumor necrosis factor receptor-associated factor 6 was increased upon the lack of ubiquitin-specific peptidase 47, a DUB, which activates nuclear factor κB (NF-κB)[14]. By precisely reversing K63-linked ubiquitination of receptor-interacting protein kinase 1 (RIPK1), ovarian tumor deubiquitinase 1, another DUB, has a suppressive impact on RIPK1-mediated activation of NF-κB, which decreases intestinal inflammation[15]. DUBs are, therefore, essential for immune cells' intestinal immunomodulatory processes, and identification of the roles of functional DUBs in inflammatory regulations may provide new targets and strategies for the treatment of IBD.

Josephin domain-containing protein 2 (JOSD2) is a member of the Machado-Joseph domain-containing protease subfamily, the smallest subfamily of DUBs. It has been reported that JOSD2 regulates cellular metabolism and tumorigenesis. Contemporary research has demonstrated that JOSD2 can significantly impact metabolic and neoplastic diseases by modulating several signaling pathways by deubiquitinating different substrate proteins, such as sarcoplasmic/endoplasmic reticulum $Ca^{2+}$ ATPase 2a (SERCA2a), Yes-associated protein (YAP)/transcriptional coactivator with PDZ-binding motif (TAZ), catenin beta-1 (CTNNB1), and a metabolic enzyme complex encompassing phosphoglycerate dehydrogenase, phosphofructokinase-1, and aldolase A[16-19]. However, the specific function of JOSD2 in maintaining intestinal homeostasis, as well as its involvement in colitis and colon cancer, has not been fully explained.

This study found a notable increase in macrophage JOSD2 levels in both human IBD and mouse colitis samples, suggesting the involvement of JOSD2 in the development of IBD. It was further found that deficiency of JOSD2 in myeloid cells exacerbated intestinal inflammation and IBD pathology in dextran sodium sulfate (DSS)-challenged mice, while overexpression of JOSD2 prevented colitis in mice caused by DSS. The deletion of JOSD2 also facilitated the development of CRC in azoxymethane (AOM)/DSS-induced mice. Mechanistically, we demonstrated that JOSD2 removed K63-linked ubiquitin from the K134 site of inosine-5′-monophosphate dehydrogenase 2 (IMPDH2), leading to the inactivation of the IMPDH2−NF-κB proinflammatory signaling pathway in macrophages. These results indicate that JOSD2 has the potential to be a target for therapeutic intervention in IBD.

## 2. Materials and methods

### 2.1. Cell culture and reagents

The cell lines HEK293T cells (Cat #: GNHu17) and L-929 cells (Cat #: GNM28) were acquired from the National Collection of

Authenticated Cell Cultures in Shanghai, China. HEK293T cells were cultivated in Dulbecco's modified Eagle's medium (DMEM; Gibco) supplemented with fetal bovine serum (FBS; 10%; Gibco, Eggenstein, Germany). L929 cells were maintained in MEM-$\alpha$ (Gibco) medium, which was enriched with FBS of the same concentration as well. The LPS (Cat #: L2880) and azoxymethane (Cat #: A5486) were obtained from Sigma−Aldrich (St. Louis, MO, USA). MG132 (Cat #: T2154) was obtained from TargetMol (Shanghai, China). The Dextran sulfate sodium (DSS; Cat #: 0216011080), with a molecular weight of 36−50 kDa, was purchased from MP Biomedicals (Aurora, OH). The anti-JOSD2 antibody (Cat #: orb184482) was obtained from Biorbyt (Cambridge, UK). The anti-IMPDH2 antibody (Cat #: PTM-6170) was obtained from PTM Biolasb (Hangzhou, China). The anti-MYC-Tag antibody (Cat #: 2276), anti-F4/80 antibody (Cat #: 70076), p-NF-$\kappa$B p65 antibody (Cat #: 3033), NF-$\kappa$B p65 antibody (Cat #: 8242), NF-$\kappa$B inhibitor $\alpha$ antibody (Cat #: 4812), glyceraldehyde-3-phosphate dehydrogenase antibody (Cat #: 5174), and HRP-linked second antibody (Cat #: 7074) were obtained from Cell Signaling Technology (Beverly, MA, USA). The anti-HA-Tag antibody (Cat #: 51064-2-AP), anti-Flag-Tag antibody (Cat #: 66008-4-Ig), anti-GFP-Tag antibody (Cat #: 66002-1-Ig), and anti-$\beta$-actin antibody (Cat #: 66009-1-Ig) were obtained from Proteintech (Wuhan, China). The anti-HA magnetic beads (Cat #: HY-K0201) were purchased from MCE Biotech (Shanghai, China). The Protein A + G Agarose (Cat #: P2055) utilized for immunoprecipitation was sourced from Beyotime (Shanghai, China). The MonoRab™ Anti-Flag Magnetic Beads (Cat #: L00835) were obtained from GenScript in Nanjing, China.

### 2.2. Plasmids construction and transfection

JOSD2-flag, JOSD2-C24A-Flag, GFP-IMPDH2-HA, GFP-ΔCBS-IMPDH2-HA, GFP-232-514-IMPDH2-HA, GFP-K124R-HA, GFP-K134R-HA, GFP-K349R-HA, GFP-K422R-HA, and GFP-K489R-HA plasmids were used in this study (Tsingke Biotechnology, Beijing, China). The plasmids Myc-Ub-K63, Myc-Ub-K48, Myc-Ub-K33, Myc-Ub-K29, Myc-Ub-K27, Myc-Ub-K11, Myc-Ub-K6, Myc-Ub-K48R, and Myc-Ub-WT were acquired for this assay (KeLei Biological Technology, Shanghai, China). By utilizing DNA sequencing, all constructions were confirmed. Using the lipofectamine 3000 reagent (Invitrogen, Carlsbad, CA, USA), the plasmids were introduced into HEK293T cells by transfection following the directions provided by the manufacturer.

### 2.3. Human samples

Quzhou People's Hospital of Wenzhou Medical University collected 10 samples of colonic biopsies from UC patients and 9 samples of colonic biopsies from CD patients who were hospitalized. An additional ten colon samples were collected from the healthy colon tissues surrounding the tumors of colon cancer patients undergoing colectomy surgery at the hospital. The studies involving human subjects underwent a thorough evaluation and received approval from the Human Ethical Committee of the Quzhou People's Hospital of Wenzhou Medical University (2022-0037) with a waiver of written informed consent, and conformed to the principles outlined in the declaration of Helsinki. The essential details of the patients, such as their age and gender, are consolidated in Supporting Information Table S1.

### 2.4. Animals

JOSD2 knockout (KO) mice (C57BL/6J background, *Josd2*$^{-/-}$) were developed from C57BL/6J mice provided by Professor Fuping You from Peking University in Beijing, China. The mice remained in a controlled environment with specific pathogen-free environments. The humidity was maintained at 50 ± 5% and the temperature at 22 ± 2 °C. The mice were provided with a 12-h/12-h light/dark cycle. The Institutional Animal Policy and Welfare Committee of Wenzhou Medical University accepted all animal research (Approval document # wydw2022-0648), which was carried out strictly as per the established guidelines of the US National Institutes of Health (Guide for the Care and Use of Laboratory Animals).

### 2.5. DSS-induced colitis and colitis-associated colorectal cancer models

For five days, 8-week-old mice (female) were given DSS (2.5%) in their water as part of the DSS-induced colitis paradigm. After that, regular drinking water was provided for two days. On the 7th day, the mice were sacrificed with anesthesia. In the survival analysis, the drinking water was treated with a 2.5% DSS solution after 6 days, and regular water was then supplied until Day 16. On Day 0 of the developed colitis-associated colorectal cancer model caused by AOM/DSS, male mice were cohoused and administered intraperitoneally (i.p.) with AOM at a dosage of 10 mg/kg in PBS. The drinking water with DSS (2.0%) was supplied for five days, afterward for fourteen days regular water was given. On Day 76, the mice were anesthetized and euthanized after three rounds of DSS treatment.

### 2.6. Isolation of murine lamina propria mononuclear cells

Murine LPMCs were isolated from 8 to 10-week-old WT and *Josd2*$^{-/-}$ mice using a digestion method, as previously described[20]. Briefly, colon tissue was cut into 5−6 cm pieces, opened longitudinally, and flushed with 1 × cold phosphate-buffered saline (PBS). The colon tissue slices were incubated in 10 mL of PBS supplemented with 0.03 mol/L ethylenediaminetetraacetic acid (EDTA) and 1 mmol/L dithiothreitol (DTT) at 4 °C for 20 min under slow rotation (50 × *g*) in an incubator in a 50 mL tube. The digested sample was incubated in 10 mL of PBS supplemented with 0.03 mol/L EDTA at 37 °C for 20 min under rotation in a 50 mL tube. After incubation, the cell solution was thoroughly vortexed for 30 s and washed with PBS to remove residual EDTA. The supernatant was used for subsequent extraction of intestinal epithelial cells. Using scissors, the remaining tissue was cut into 1 mm pieces. The tissue was collected into 50 mL tubes containing 10 mL of DMEM supplemented with 1 mg/mL of collagenase D (Roche) and 0.1 mg/mL of DNase I (Roche). For digestion, the pieces were incubated at 37 °C for 60 min with gentle shaking. After incubation, cells were passed through a 100-mm nylon mesh (BD Biosciences) and centrifuged at 1500 × *g* for 8 min at 4 °C. The supernatant was discarded and the pellet was resuspended in Fluorescent Activated Cell Sorting (FACS) buffer and then stained for flow cytometric analysis.

### 2.7. Isolation of murine intestinal epithelial cells

Murine intestinal epithelial cells (IECs) were isolated from 8 to 10-week-old WT and *Josd2*$^{-/-}$ mice using a digestion method, as previously described[21]. Briefly, colon tissue was cut into 5−6 cm pieces, opened longitudinally, and flushed with 1 × cold PBS. The colon tissue slices were incubated in 10 mL of PBS supplemented with 0.03 mol/L EDTA and 1 mmol/L DTT at 4 °C for 20 min under slow rotation (50 × *g*) in an incubator in a 50 mL tube. The digested sample was incubated in 10 mL of PBS supplemented with 0.03 mol/L EDTA at 37 °C for 20 min under rotation in a 50 mL tube. After incubation, the cell solution was thoroughly vortexed for 60 s and washed with PBS to remove residual EDTA. The supernatant was used for subsequent extraction of IECs. The cells were washed in 10 mL DPBS with 10% FBS, dissociated with 8 mg dispase for 8 min at 37 °C in a water bath and stopped by adding 10% FBS and 50 μL of 10 mg/mL DNase to the cell solution. Then, cells were centrifuged at 1000 × *g* for 5 min at 4 °C. The pellet was resuspended in 10 mL HBSS with 10% FBS and centrifuged at 1000 × *g* for 5 min at 4 °C. The supernatant was discarded and the pellet was used for Western blot analysis.

### 2.8. Isolation of bone marrow-derived macrophages and mouse peritoneal macrophages

Using the technique described in a previously reported work, primary bone marrow-derived macrophages (BMDMs) were isolated from the tibia and femur of mice[22]. In summary, the femur and tibia were cleaned using RPMI 1640 solution containing 100 units/mL of penicillin and 100 μg/mL of streptomycin. Next, the samples underwent filtration using nylon mesh (70 mm). Following centrifugation (1200 × *g*; 5 min) and extraction, bone marrow cells were cultured in DMEM supplemented with 10% FBS and 20% L-929 culture medium. The medium was introduced on the third and 5th days. On the 7th day, cells were utilized for experimental purposes. Primary mouse peritoneal macrophages (MPMs) were isolated from 8-week-old WT mice, as previously described[23].

### 2.9. Bone marrow chimeric mouse model

Previously documented methods were used to create bone marrow chimeric mice [22]. The mice who received the treatment were exposed to radiation at a dosage of 6 Gy. From either wild-type (WT) or *Josd2*$^{-/-}$ KO mice, cells from bone marrow were collected. Each radiation-exposed WT mouse underwent an intravenous infusion of 5.0 × $10^6$ bone marrow cells from the donor *via* the tail vein. Following 8 weeks, colitis induced *via* DSS was administered to the WT → WT and KO → WT mice.

### 2.10. Histological analysis

After being submerged in a solution containing 4% paraformaldehyde, the colon tissues were fixed and paraffin-embedded. Next, 5 μm colon sections were generated, which were treated to remove wax and rehydrated were analyzed using hematoxylin and eosin (H&E) staining to evaluate the extent of colon damage and the level of inflammation. Two investigators assessed the pathogenic scores of inflamed colons in a blinded manner by combining the histology and disease activity index (DAI) scores. To gauge the severity of colitis, the DAI score was calculated for each mouse as a cumulative value. The evaluation was based on weight loss, with a scoring scale of 0 for no weight loss, 1 for 1%−5% weight loss, 2 for 6%−10% weight loss, 3 for 11%−18% weight loss, and 4 for greater than 18% weight loss. There were four categories for evaluation of stool consistency, where 0 indicates stool with normal consistency, 1 shows stool that is soft but still formed, 2 indicates stool that is soft and loose, 3 shows stool that is extremely soft and wet, and 4 indicates watery diarrhea. A score of 0 suggests there is no blood in the stool, 1 and 2 indicate focal bloody feces, 3 shows there are traces of blood in the stool, and 4 indicates severe rectal bleeding. A cumulative scoring method was employed to evaluate the histological alterations. Four scores were assigned based on the degree of epithelial damage: 0 for normal morphology, 1 for goblet cell loss, 2 for goblet cell loss in large regions, 3 for crypt loss, and 4 for crypt loss in large areas. Furthermore, the degree of infiltration of inflammatory cells was graded as follows: 0 represented no infiltration, 1 the infiltration surrounding the crypt bases, 2 the infiltration spreading to the muscularis mucosa, 3 the extensive infiltration in the muscularis mucosa accompanied by a large amount of edema, and 4 the infiltration spreading to the submucosa. These scoring criteria have been previously described[24].

### 2.11. Immunohistochemistry

The sections were subjected to wax removal and were rehydrated before the antigen retrieval procedure. The sections were placed in the water bath (boiling) in 0.01 mol/L citrate buffer with pH 6.0 for 2 min to retrieve the antigens. Then, the activity of endogenous peroxidases was inhibited by treating the sections with 0.3% hydrogen peroxide for 10 min. Subsequently, the sections were immersed for 30 min in normal goat serum (5%; Solarbio, Beijing, China). After that, the sections were left at room temperature for 2 h with the primary antibodies (F4/80; 1:400). DAB and secondary antibodies coupled with HRP were used for chromogenic visualization. The portions were then sealed with neutral gum after dehydrating with an alcohol gradient. The epifluorescence microscope and digital camera (Nikon, Tokyo, Japan) were utilized to acquire the pictures under bright-field illumination. In a blinded fashion, two researchers independently assessed the percentages of colonic samples that had positive staining for JOSD2. Periodic acid-Schiff/Alcian blue staining (PAS/AB; Solarbio, Beijing, China) was used to assess goblet cells. The Beyotime kit (Cat #: C1086) was used to carry out the TUNEL staining process. The ImageJ program (1.38e; National Institutes of Health in Bethesda, MD, USA) was used to quantify the positive area of TUNEL labeling, F4/80 staining, and PAS/AB staining.

### 2.12. Immunofluorescence microscopy

After fixing frozen sections with 4% paraformaldehyde for 15 min, primary antibodies were applied and left overnight. Next, the sections were treated with secondary antibodies conjugated with the appropriate fluorophore for 1 h at 37 °C. The following were the primary antibodies: JOSD2 (Cat #: orb184482, 1:400, Biorbyt) and CD68 (Cat #: 66231-2-Ig, 1:3000, Proteintech). The nuclei were stained with DAPI to make them visible. Using a fluorescent microscope and Olympus's DP2-BSW software (2.2), immunofluorescence pictures were captured.

### 2.13. Enzyme-linked immunosorbent assay

The colon tissue supernatant was obtained by homogenizing the tissue obtained from mice treated with water or DSS to form lysate. Using the interleukin-1$\beta$ (IL-1$\beta$) Mouse ELISA Kit (Cat #:

88-7013-77, ThermoFisher, Carlsbad, CA, USA) and the interleukin-6 (IL-6) ELISA Kit (Cat #: 88-7064-77, ThermoFisher, Carlsbad, CA, USA), the cytokine levels were measured.

### 2.14. Co-immunoprecipitation

The cells that had undergone transfection were lysed on ice using NP-40 Lysis Buffer, composed of 150 mmol/L NaCl, 50 mmol/L Tris−HCl (pH 7.4), and 1% NP-40, along with a protease inhibitor cocktail (Cat #: P1045, Beyotime). The resulting mixture was then subjected to sonication for 1 min, followed by 12,000 × *g* centrifugation for 15 min at 4 °C. One-tenth of the volume of the supernatant was kept as input. At the same time, the rest was subjected to overnight incubation on a rotator at 4 °C with either anti-HA magnetic beads or anti-Flag magnetic beads. After that, the immunocomplexes were extracted using sodium dodecyl sulfate (SDS) buffer and washed five times with 500 μL of lysis buffer.

### 2.15. Western blot analysis

The cells and the colon tissues were homogenized using RIPA buffer (Cat #: P0013B, Beyotime) that contained a mixture of phosphatase inhibitors and protease (Cat #: P1051, Beyotime). The quantification of proteins was done using a Quick Start™ Bradford Protein Assay Kit (Bio-Rad, Hercules, CA, USA). Approximately 35 μg protein was used and electrophoresed in SDS−polyacrylamide gels electrophoresis, then transferred to a polyvinylidene difluoride membrane. Subsequently, the membranes were treated for an hour with 5% skim milk to accomplish blocking and then left for incubation with primary antibodies overnight. A ChemiDoc XRS + system (Bio-Rad) detected discrete protein bands after incubation with HRP-conjugated secondary antibodies.

### 2.16. RNA extraction and quantitative real-time PCR

BMDM cells and mouse colon tissues were lysed to extract total RNA using TRIzol (Invitrogen). TransScript® All-in-One First-Strand cDNA Synthesis SuperMix (TransGen Biotech, Beijing, China) was utilized to synthesize cDNAs. PerfectStart® Green qPCR SuperMix from TransGen Biotech (Beijing, China) was used in the RT-qPCR analysis, which was performed with the CFX96 Touch Real-Time PCR Detection System (Bio-Rad). Supporting Information Table S2 contains the primer sequences.

### 2.17. Enzyme assay

Enzyme assay was established as previously described[25]. The experiment was conducted using a 96-well UV plate (Costar, 3635) with a final volume of 200 μL. The reaction buffer, consisting of 3 mmol/L EDTA, 100 mmol/L KCl, 50 mmol/L Tris−HCl (pH 8.0), and 1 mmol/L dithiothreitol, was added in a quantity of 100 μL each well. Additionally, 100 μL of protein solution was added to each well, derived from a stock concentration of 5 mg/mL. The reaction was started by adding 300 mmol/L of IMP and 500 mmol/L of $NAD^+$ to the test solution for 50 min at 37 °C. To halt the reaction, 15 mmol/L of GMP was added. The NADH produced was quantified by measuring the absorbance at 340 nm using the SpectraMax iD3 System (Molecular Devices).

### 2.18. Adeno-associated virus 6 construction and injection

The AAV6 delivery system with CD68 promoter was used to overexpress JOSD2 in the macrophages of mice, as described previously[26]. The transgene plasmids used were pAAV6-CD68p-JOSD2-EGFP (AAV6-JOSD2) and control plasmid were generated by Shanghai Genechem Co., Ltd. (Shanghai, China). Mice were injected *via* the tail vein with 200 μL of virus containing $1 \times 10^{11}$ vg of the AAV6 vector genomes.

### 2.19. Statistical analyses

The findings were represented as the mean ± standard deviation (SD). The data was analyzed *via* GraphPad Prism 8. The Kolmogorov−Smirnov test verified the conformity of data to a normal distribution. The Student's *t*-test compared two sets of data in this study. A one-way analysis of variance (ANOVA) was conducted, with Dunnett's *post hoc* test, for comparison of more than two groups. Kaplan−Meier survival curves were created for the mouse survival research, and a log-rank test was used to assess the statistical significance. A significance level of $P < 0.05$ was used. Post-tests were conducted when the attained *F*-value was less than 0.05, indicating statistical significance and no significant variation in inhomogeneity. After assessing the data distribution's normality and variance, the statistical tests were judged suitable. There was no data point exclusion or randomization used. There was no "blinding" of the investigators.

## 3. Results

### 3.1. JOSD2 expression is upregulated in both patients and mice with colitis

To investigate the role of JOSD2 in IBD, we first searched the open-access integrated Gene Expression Database (GEO) and found that the transcription of JOSD2 in colon tissues of patients with IBD (GSE179128) was significantly higher than that in healthy human colon tissues (Fig. 1A, left). Similarly, another GEO database (GSE123141), in which the samples were from the intestinal macrophages of UC patients and normal controls, showed that the transcription of JOSD2 in macrophages from UC patients was higher than that from normal controls (Fig. 1A, right). The other members of the MJD family were also searched, and the result showed that mRNA levels of *JOSD1* and ataxin-3 (*ATXN3*) were not significantly changed in the GEO database (Supporting Information Fig. S1A and S1B). Next, the expression of JOSD2 and CD68 in colon samples from UC or CD patients was analyzed. JOSD2 was co-localized with the macrophage marker CD68 in IBD human intestines (Fig. 1B). It was found that the expression of JOSD2 in colon tissues was significantly increased in patients with UC or CD than that in individuals without IBD (Fig. 1B and C).

Consistent with the transcriptome sequencing data of patient colons, mRNA levels of *JOSD2* in colon tissues from mice with DSS-treated colitis were higher ($P = 0.0005$) than those from the controls, while mRNA levels of *JOSD1* and *ATXN3* were not significantly altered in mice with colitis (Fig. 1D). Furthermore, the expression of JOSD2 in colon tissue was assessed using immunohistochemical (IHC), immunofluorescence and Western blot analysis, and results reveal that the expression of JOSD2 and CD68 in colon tissues from mice with colitis were higher than

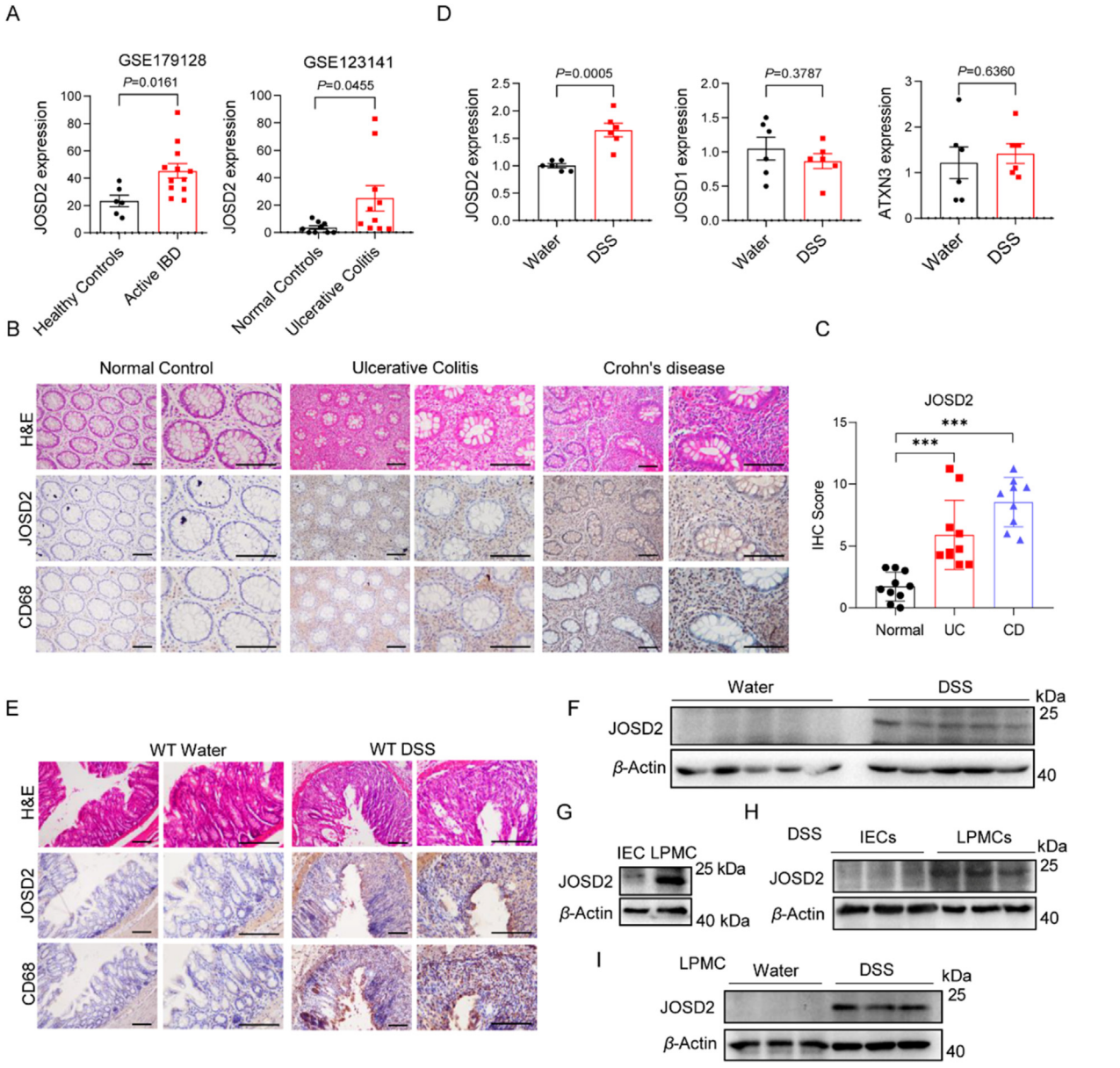


**Figure 1** Increased JOSD2 expression in inflamed intestinal tissues from UC patients and mice with colitis. (A) mRNA levels of *Josd2* in colon mucosal tissues of healthy controls and patients with active IBD (GSE179128). mRNA levels of *Josd2* in colonic macrophage of normal controls and ulcerative colitis (UC) patients (GSE132141). (B) Representative images of H&E staining and immunohistochemical (IHC) staining of JOSD2 and CD68 in colon biopsy samples obtained from patients with UC, Crohn's disease (CD) and normal adjacent colon tissues obtained from colon cancer patients admitted for CRC surgery. Scale bar = 100 μm. (C) JOSD2 IHC score between the three groups is shown. (D) mRNA levels of *Josd2*, *Josd1*, *ATXN3* in colon mucosal tissues of the control and DSS-induced colitis. (E) Representative images of H&E staining and IHC staining for JOSD2 and CD68 in the colonic samples from control and mice with DSS-induced colitis. Scale bar = 100 μm. (F) Immunoblot analysis of JOSD2 in the distal colons of the control and DSS-induced colitis. β-Actin was used as the loading control ($n = 5$). (G) Immunoblot analysis of JOSD2 in IEC and LPMC isolated from the control mice. β-Actin was used as the loading control. (H) Immunoblot analysis of JOSD2 in IECs and LPMCs isolated from the DSS-induced mice. β-Actin was used as the loading control ($n = 3$). (I) Immunoblot analysis of JOSD2 in LPMCs isolated from the controls and the DSS-induced mice. β-Actin was used as the loading control ($n = 3$). Statistical data are shown as mean ± SD; $^{***}P < 0.001$.

those from the controls (Fig. 1E and F, and Supporting Information Fig. S2). Western blot analysis also showed that the expression of JOSD2 was mainly in murine lamina propria mononuclear cells (LPMCs), rather than intestinal epithelial cells IECs under either physiological condition or inflammatory conditions (Fig. 1G and H). As JOSD2 was mainly located in macrophages, LPMCs were isolated from control- and DSS-treated mouse colons, and it was found that JOSD2 protein expression was significantly increased in the DSS group compared with the control group (Fig. 1I). Collectively, these results suggest

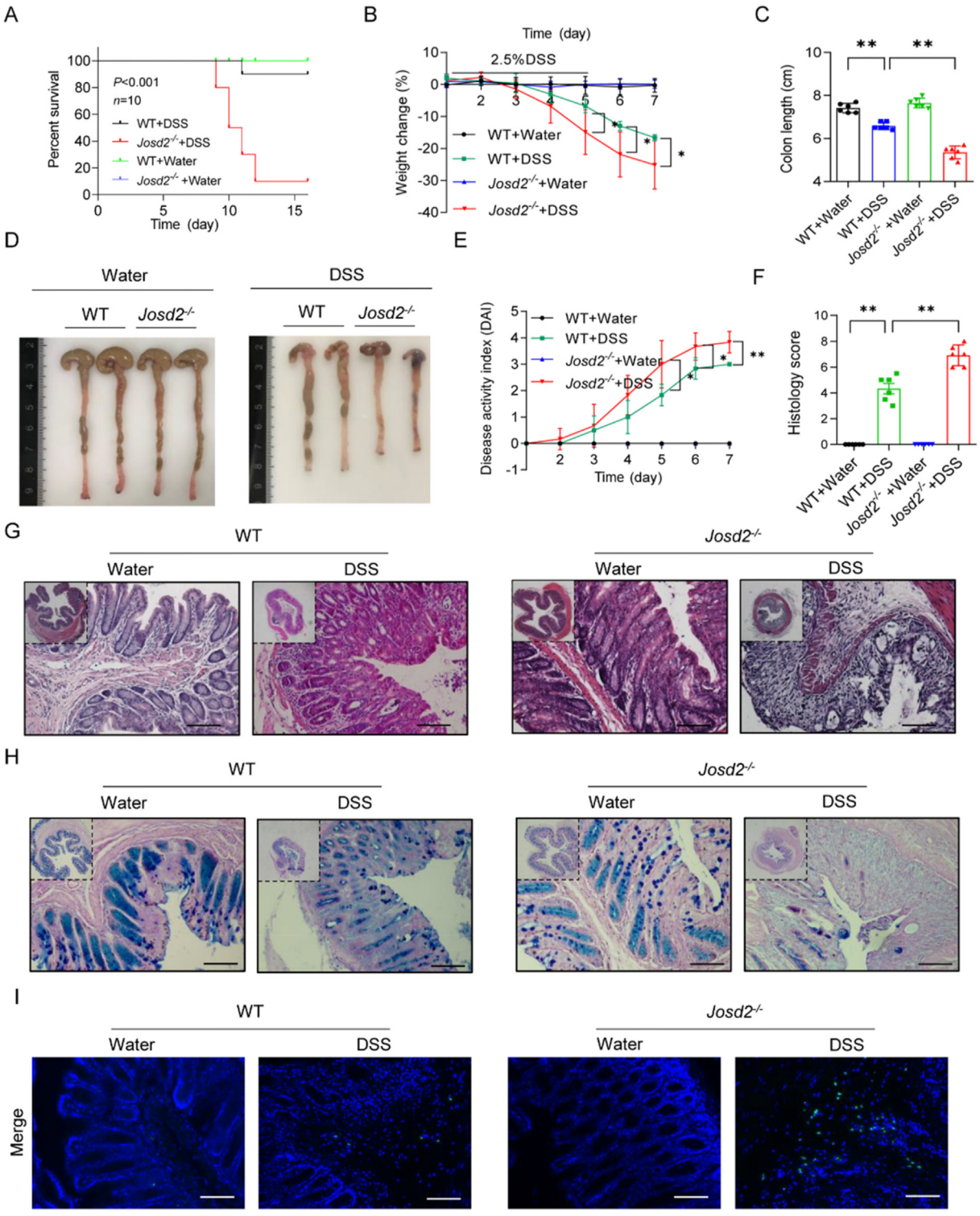


**Figure 2** JOSD2 deficiency exacerbates colonic injury induced by DSS-induced colitis. (A) Survival (Kaplan−Meier) curves ($n = 10$) of WT and *Josd2*$^{-/-}$ mice with 2.5% DSS-induced colitis. (B) Body weight change ($n = 6$) of WT and *Josd2*$^{-/-}$ mice with 2.5% DSS-induced colitis. Colon length (C) and representative images of colon tissues (D) from the indicated treatment groups on Day 7 after DSS treatment ($n = 6$). Disease activity index (E) and semi-quantitative scoring of histopathology on Day 7 after DSS administration (F) are shown ($n = 6$). Representative images of H&E (G) PAS/AB (H) and TUNEL (I) staining in cross-sections of distal colon tissues from WT and *Josd2*$^{-/-}$ mice on Day 7 after DSS administration. Scale bar = 100 μm. Statistical data are presented as mean ± SD. *$P < 0.05$, **$P < 0.01$.

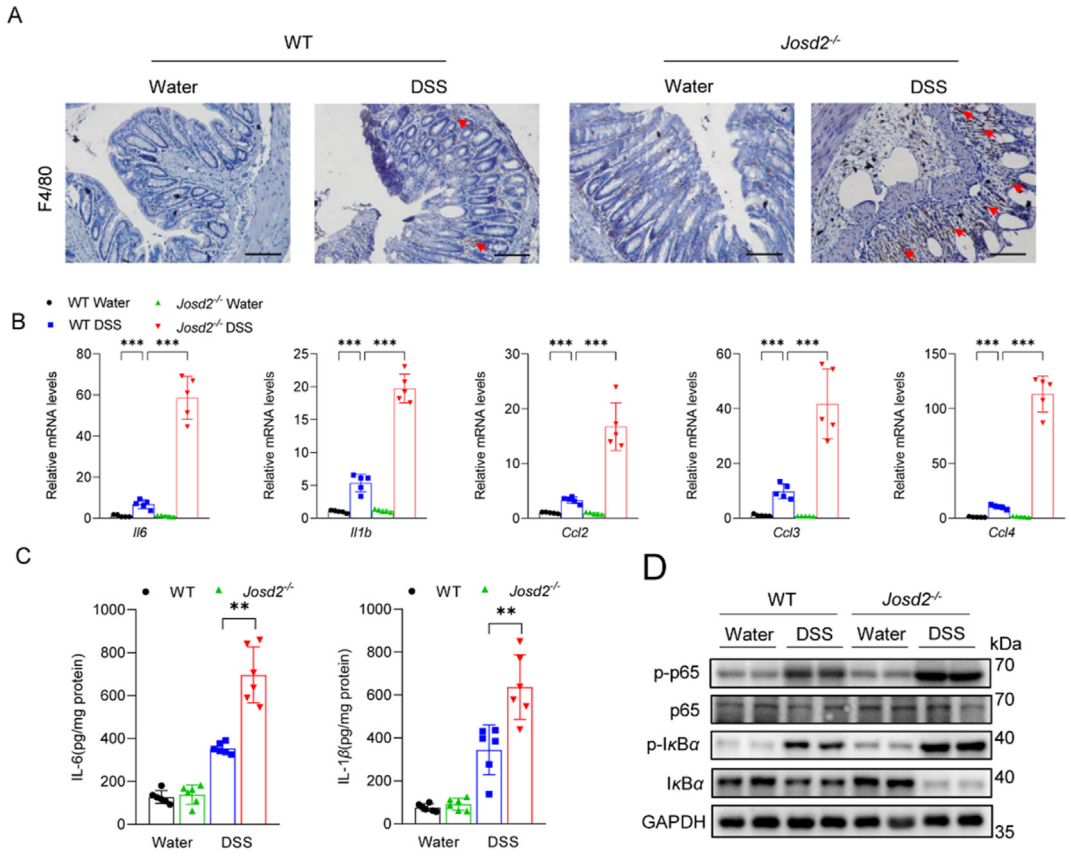


**Figure 3** JOSD2 deficiency increases the inflammatory infiltration and production of proinflammatory cytokines. (A) Representative images of F4/80 staining in cross-sections of distal colon from WT and *Josd2*$^{-/-}$ mice on Day 7 after DSS administration. Scale bar = 100 μm. (B) mRNA levels of the proinflammatory genes in colon sections from WT and *Josd2*$^{-/-}$ mice after DSS treatment ($n$ = 5). (C) IL-6 and IL-1$\beta$ levels in colon tissues from WT and *Josd2*$^{-/-}$ mice treated with 2.5% DSS were measured *via* ELISA ($n$ = 6). (D) Representative Western blot analysis of total and phosphorylated p65 and IκBα in the colons of mice from the indicated groups. Glyceraldehyde-3-phosphate dehydrogenase (GAPDH) served as the loading control. Data are presented as mean ± SD. *$P$ < 0.05, **$P$ < 0.01, and ***$P$ < 0.001.

that increased JOSD2 expression in macrophages is correlated with colonic injuries in both humans and mice.

### 3.2. *JOSD2 deficiency exacerbates DSS-induced colitis in mice*

In order to examine the function of JOSD2 in DSS-induced colitis, the age- and sex-matched wild-type (WT) mice and mice lacking the *Josd2* gene (*Josd2*$^{-/-}$) to generate acute colitis using DSS were utilized. As shown in Supporting Information Fig. S3, DNA electrophoresis and Western blot confirmed the knockout efficiency of JOSD2 in mice. According to the data presented in Fig. 2A, the *Josd2*$^{-/-}$ mice survival rate was considerably lower compared to that of WT littermates following 2.5% DSS administration ($P < 0.001$). Subsequently, mice of the WT and *Josd2*$^{-/-}$ genotypes were subjected to treatment with a 2.5% DSS solution to evaluate the involvement of JOSD2 in the progression of IBD. When comparing *Josd2*$^{-/-}$ animals to WT mice, it was seen that *Josd2*$^{-/-}$ mice had more severe colitis symptoms. This was shown by a more significant weight loss (Fig. 2B) and shorter colon tissues (Fig. 2C and D). Furthermore, *Josd2*$^{-/-}$ mice exhibited more severe colitis symptoms, such as decreased stool consistency and rectal hemorrhage, leading to a higher DAI in comparison to the WT mice (Fig. 2E). Additional histological analysis demonstrated that *Josd2*$^{-/-}$ animals displayed a much more damaged colon epithelial barrier and a higher number of ulcerations upon comparison to WT mice following DSS therapy (Fig. 2F and G). Moreover, the PAS-AB staining technique showed that *Josd2*$^{-/-}$ mice had a lower number of goblet cells compared to WT mice following DSS administration, as seen in Fig. 2H and Supporting Information Fig. S4A. The TUNEL labeling results indicated that *Josd2*$^{-/-}$ animals exhibited a higher number of apoptotic cells in their colon tissues than WT mice following DSS administration (Fig. 2I and Fig. S4B). Taken together, these data suggest that JOSD2 deficiency significantly exacerbates DSS-induced colon injuries.

### 3.3. *JOSD2 deficiency increases the production of inflammatory cytokines in DSS-challenged mice*

In order to ascertain the role of JOSD2 in regulating the inflammatory reaction in DSS-induced colitis, the extent of inflammatory cell infiltration in the colon tissues was initially evaluated. The observations indicated that the F4/80 level in *Josd2*$^{-/-}$ mice's colons was much higher than in WT mice following the administration of DSS. This suggests that the absence of JOSD2 worsened the infiltration of immune cells in colon tissues generated by DSS (Fig. 3A and Fig. S4C). Corroborating these findings, the levels of proinflammatory cytokines and chemokines mRNA were

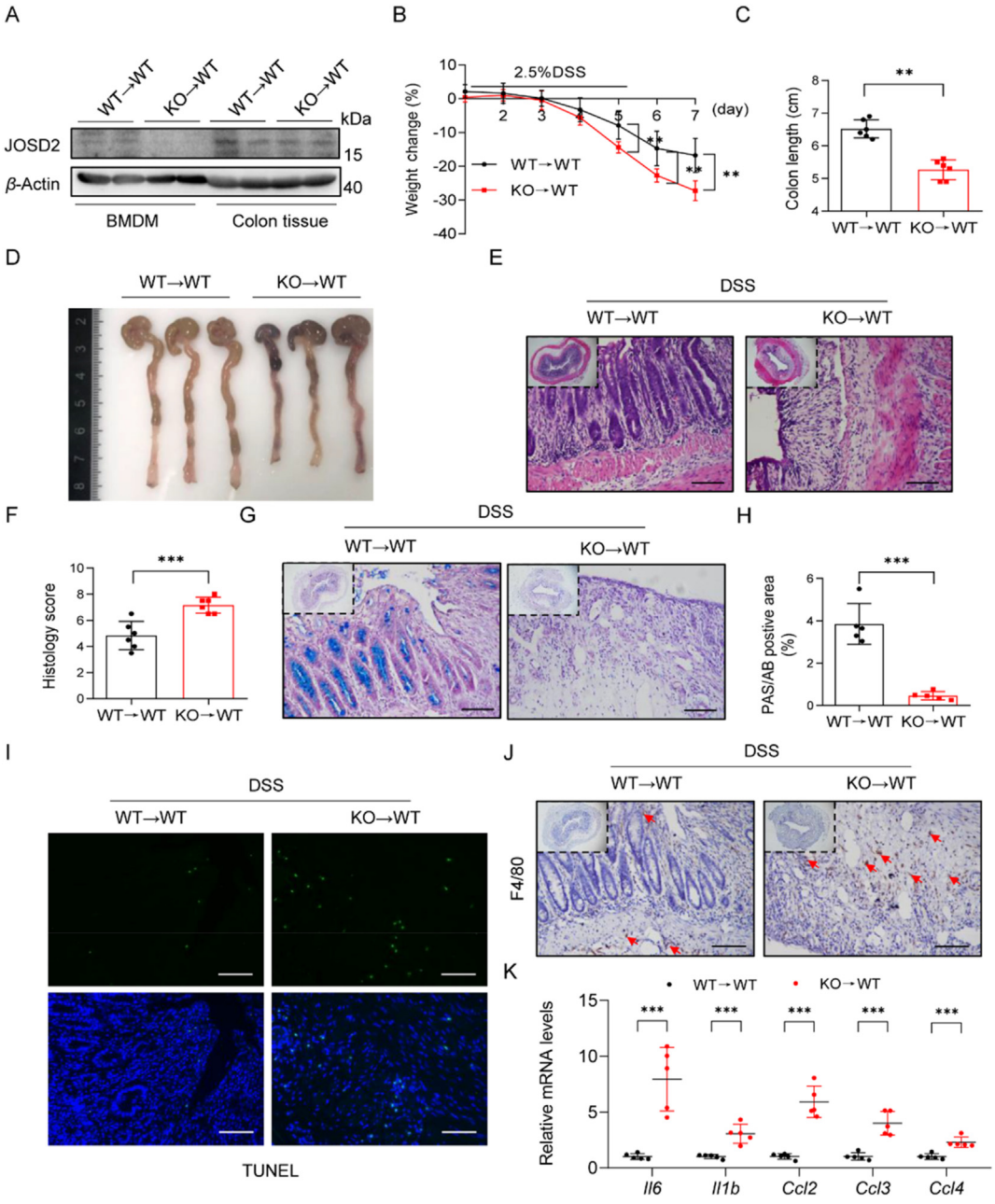


**Figure 4** Deficiency of JOSD2 in myeloid cells exacerbates DSS-induced colitis. (A) Bone marrow derived macrophages (BMDMs) and colon tissues were obtained from chimeric mice 8 weeks after the transplantation of bone marrow cells. Levels of JOSD2 protein were probed through immunoblotting. $\beta$-Actin was used as the loading control. (B) Two groups of chimeric mice (WT→WT and KO→WT) generated by bone marrow transplantations were exposed to 2.5% DSS for 5 days and followed by 2 days regular drinking water, and body weight changes were daily monitored ($n = 6$). (C, D) Representative images of colons and colon length from the two groups on Day 7 after DSS treatment ($n = 6$). (E−H) Representative images of H&E (E) and PAS/AB staining (G) in distal colon cross-sections and semi-quantitative scoring of histopathology (F) and quantification of PAS/AB staining area (H) ($n = 5$−6), scale bar = 100 μm. (I, J) Representative images of TUNEL (I) and F4/80 staining (J) in distal colon cross-sections of chimeric mice described in D. (K) mRNA levels of the proinflammatory genes in colon sections from WT→WT and KO→WT mice after DSS treatment ($n = 5$). Data are presented as mean ± SD. $^{**}P < 0.01$, and $^{***}P < 0.001$.

markedly elevated in the colon tissues of *Josd2*$^{-/-}$ animals than those of WT, as observed in Fig. 3B. Subsequently, the protein levels of IL-6 and IL-1$\beta$, which are prominent cytokines involved in IBD was assessed[27]. The findings demonstrated that the treatment of DSS significantly elevated IL-6 and IL-1$\beta$ in the colon tissues. The alterations were improved significantly in the *Josd2*$^{-/-}$ mice than their WT littermates, as seen in Fig. 3C. The NF-$\kappa$B signaling levels in colon tissues from both WT and *Josd2*$^{-/-}$ mice were examined following the DSS challenge. The findings indicated that levels of phosphorylated-p65 and phosphorylated-I$\kappa$B$\alpha$ were markedly elevated in *Josd2*$^{-/-}$ mice upon comparison to WT mice, as seen in Fig. 3D). Collectively, these results suggest that

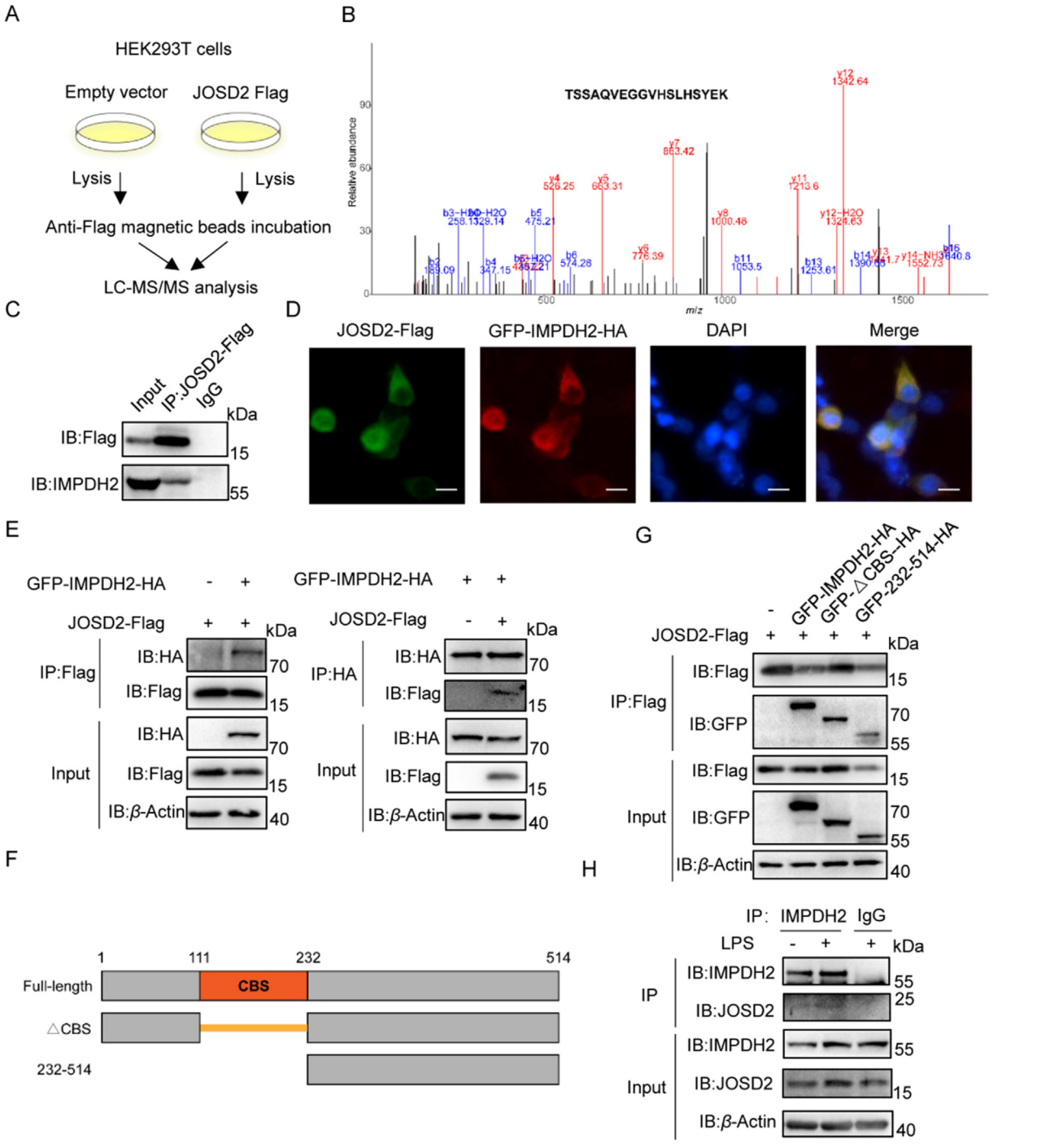


**Figure 5** JOSD2 directly interacts with IMPDH2. (A) Schematic of the experimental procedure used to identify the JOSD2 substrate screening. (B) Mass spectrum showing the structural diagram of the IMPDH2 protein. (C) Co-IP assays showed that JOSD2 interacted with IMPDH2 in HEK293T cells. Immunoprecipitations were performed using anti-FLAG magnetic beads. (D) Colocalization between JOSD2 and IMPDH2 was examined by fluorescence microscopy in HEK293T cells. (E) Immunoprecipitation analysis of the interaction of JOSD2 with IMPDH2 by anti-Flag magnetic beads or anti-HA magnetic beads, using GFP-IMPDH2-HA and JOSD2-Flag co-transfected into HEK293T cells. (F) Schematic diagram of IMPDH2 and its truncated mutants. (G) HA-tagged IMPDH2 or its truncated mutants transfected into HEK293T cells with Flag-tagged JOSD2. The cell lysates were immunoprecipitated with anti-HA magnetic beads and then immunoblotted with the indicated antibodies. (H) IP analysis of endogenous interaction of JOSD2 and IMPDH2 in LPS-stimulated BMDMs. For all immunoblot data, similar results were obtained from three independent experiments.

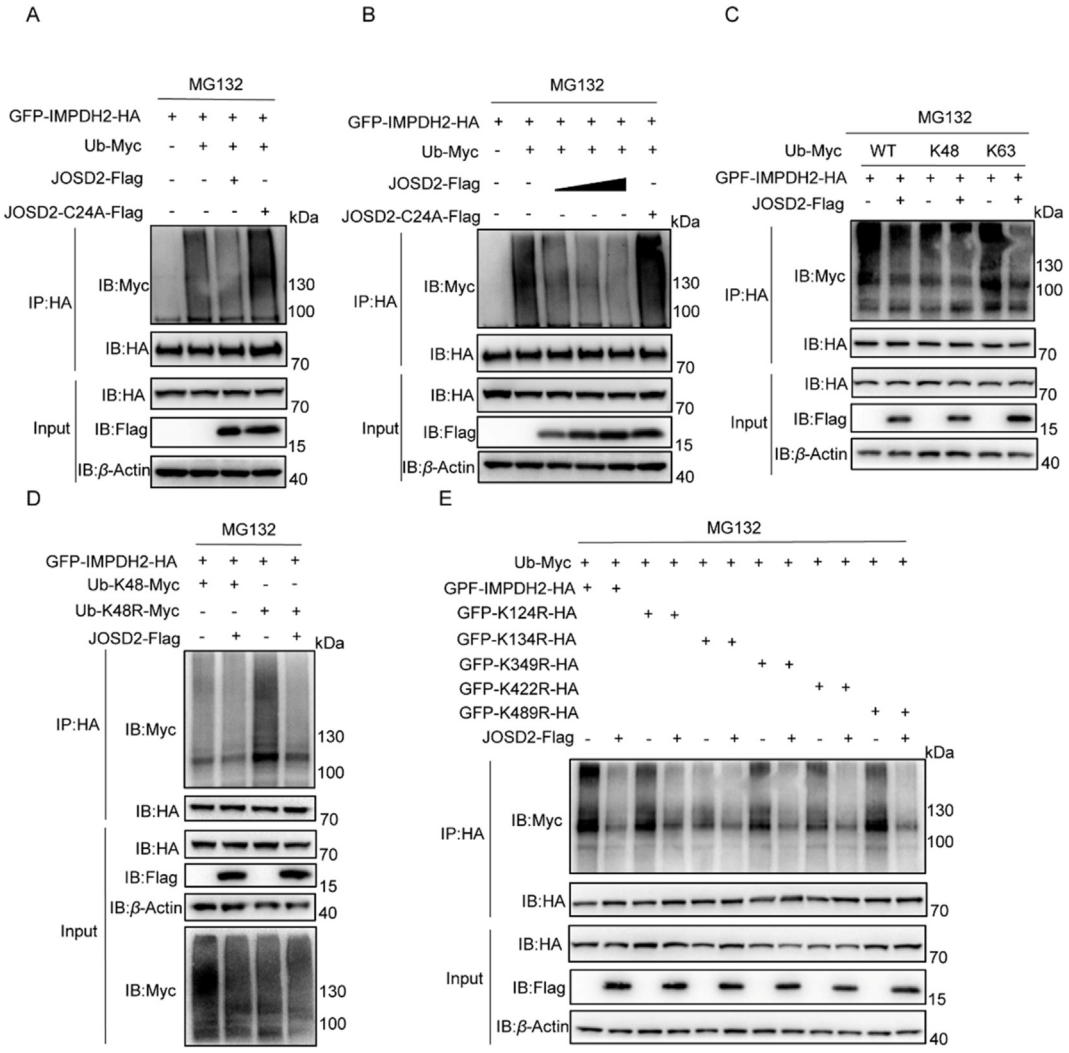


**Figure 6** JOSD2 mediates K63-linked deubiquitination of IMPDH2 at K134. (A) Immunoblot analysis of the ubiquitination of IMPDH2 in HEK293T cells co-transfected with Ub-Myc, GFP-IMPDH2-HA together with JOSD2-Flag or JOSD2-C24A-Flag, followed by IP with anti-HA magnetic beads. Cells were pretreated with 10 μmol/L of MG132 for 6 h before harvesting. (B) Immunoblot analysis of the ubiquitination of IMPDH2 in HEK293T cells co-transfected with Ub-Myc, GFP-IMPDH2-HA and increasing concentrations of vectors for the JOSD2-Flag. Cells were pretreated with 10 μmol/L of MG132 for 6 h before harvesting. (C) Immunoblot analysis of the ubiquitination of IMPDH2 in HEK293T cells co-transfected with GFP-IMPDH2-HA, JOSD2-Flag, and various types of Ub-Myc including WT, K48-, and K63-linked ubiquitin chains for 24 h and then followed by IP with anti-HA magnetic beads. Cells were pretreated with 10 μmol/L of MG132 for 6 h before harvesting. (D) Immunoblot analysis of the ubiquitination of IMPDH2 in HEK293T cells co-transfected with GFP-IMPDH2-HA, JOSD2-Flag, Ub-K48-Myc or Ub-K48R-Myc, followed by IP with anti-HA magnetic beads. Cells were pretreated with 10 μmol/L of MG132 for 6 h before harvesting. (E) Immunoblot analysis of the ubiquitination of IMPDH2 in HEK293T cells co-transfected with Ub-Myc, JOSD2-HA and GFP-IMPDH2-HA WT, or the indicated mutants. For all immunoblot data, similar results were obtained from three independent experiments.

JOSD2 deficiency increases intestinal inflammatory responses in DSS-challenged mice.

### *3.4. JOSD2 expressed in myeloid cells is responsible for protection of DSS-induced colitis*

Given the elevated JOSD2 expression in intestinal macrophages, it was postulated that JOSD2 in macrophages could primarily assist in the development of inflammatory colitis. In order to verify the function of JOSD2 in macrophages, bone marrow transplantation was performed using WT and *Josd2*$^{-/-}$ mice to generate mice with myeloid cell-specific *Josd2*$^{-/-}$. The verification of bone marrow transplantation in chimera mice is shown in Fig. 4A. According to the present study, comparing to the radiation-exposed WT mice getting WT bone marrow cells (WT → WT), KO → WT animals receiving *Josd2*$^{-/-}$ bone marrow cells had a more pronounced colitis phenotype. This was demonstrated by a higher degree of loss in body weight with a shorter colon length, as shown in Fig. 4B−D. Additionally, the use of H&E and PAS/AB staining revealed that the villi of the KO → WT mice had elevated levels of epithelial cell injury, infiltration of inflammatory cells, and a reduced number of goblet cells (Fig. 4E−H). Furthermore, the results of TUNEL labeling revealed that myeloid-specific *Josd2*$^{-/-}$ mice exhibited a higher number of

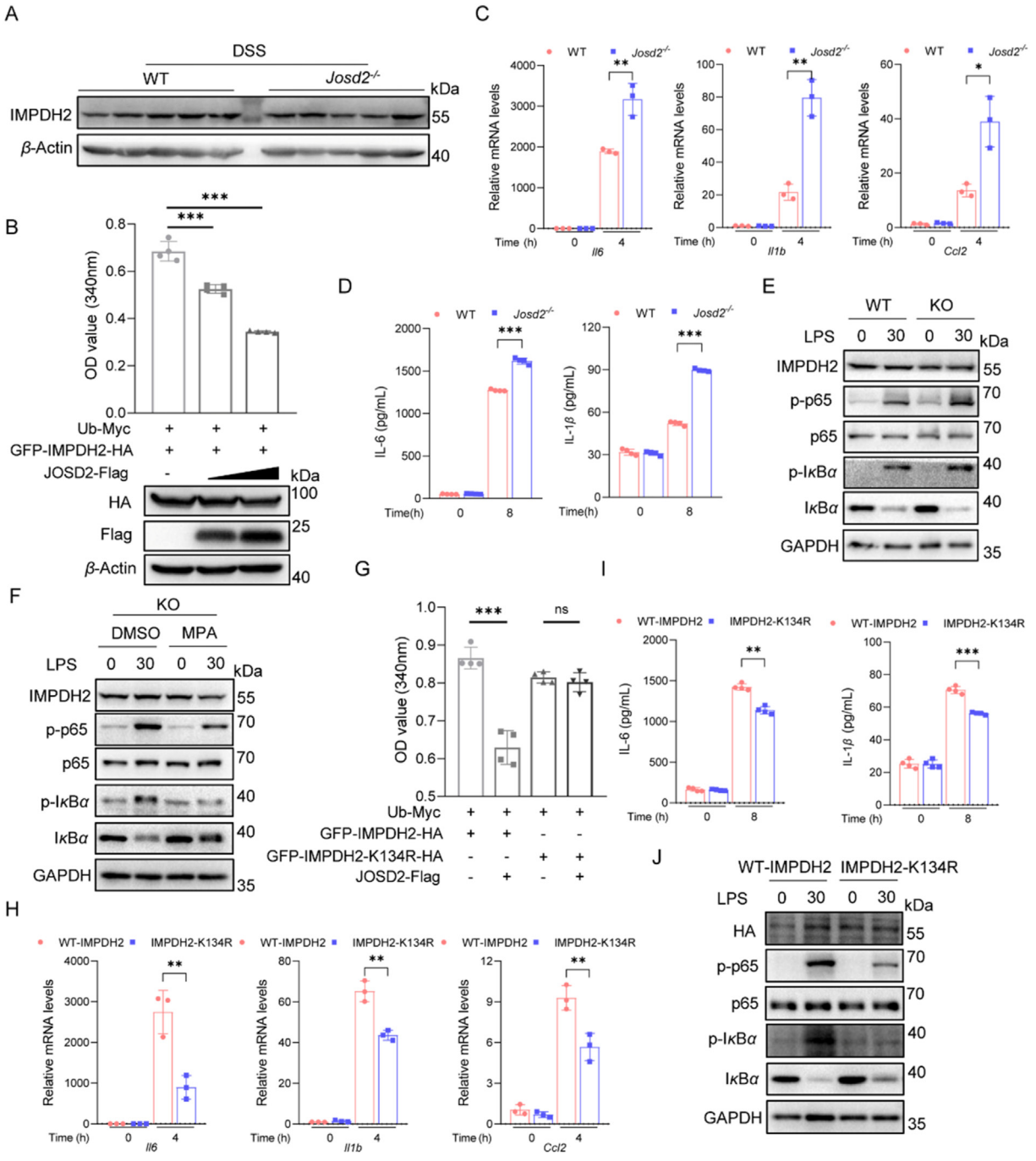


**Figure 7** JOSD2 inhibits the activity of IMPDH2 and NF-B activity. (A) Immunoblot analysis of IMPDH2 in the distal colons of the control and DSS-treated mice. $\beta$-Actin was used as the loading control ($n = 5$). (B) Enzyme activity analysis and Western blot of IMPDH2 in HEK293T cells co-transfected with Ub-Myc, GFP-IMPDH2-HA and increasing concentrations of vectors for the JOSD2-Flag. Cells were pretreated with 10 μmol/L of MG132 for 6 h before harvesting. (C) BMDMs ($1 \times 10^6$) from WT and *Josd2*$^{-/-}$ mice were treated with LPS (100 ng/mL) for 4 h. Messenger RNA levels of *Il6*, *Il1b*, and *Ccl2* were measured ($n = 3$). (D) IL-6 and IL-1$\beta$ levels in supernatants from WT and *Josd2*$^{-/-}$ BMDMs ($1 \times 10^6$) treated with LPS (100 ng/mL) for 8 h ($n = 4$). (E) BMDMs were prepared from WT and *Josd2*$^{-/-}$ mice. Cells were treated with LPS (100 ng/mL) for 30 min. Lysates then were probed for activation of downstream NF-$\kappa$B pathway proteins. Total proteins and GAPDH were used as control. (F) BMDMs were prepared from *Josd2*$^{-/-}$ mice. Cells were pretreated with 10 μmol/L IMPDH2 inhibitor mycophenolic acid (MPA) or DMSO for 4 h followed by treatment with LPS (100 ng/mL) for 30 min. Lysates then were probed for activation of downstream NF-$\kappa$B pathway proteins. Total proteins and GAPDH were used as control. (G) Enzyme activity analysis of IMPDH2 in HEK293T cells co-transfected with Ub-Myc, GFP-IMPDH2-HA, GFP-IMPDH2-K134R-HA and JOSD2-Flag. Cells were pretreated with 10 μmol/L of MG132 for 6 h before harvesting ($n = 4$). (H) BMDMs ($1 \times 10^6$) from WT mice were transfected with GFP-IMPDH2-HA or GFP-IMPDH2-K134R-HA expressing plasmid. Cells then were treated with LPS (100 ng/mL) for 4 h mRNA levels of *Il6*, *Il1b*, and *Ccl2* were measured ($n = 3$). (I) IL-6 and IL-1$\beta$ levels in supernatants from WT BMDMs ($1 \times 10^6$) transfected with GFP-IMPDH2-HA or GFP-IMPDH2-K134R-HA expressing plasmid. Cells then were

apoptotic cells in their colon tissues compared to mice with normal Josd2 levels following DSS administration (Supporting Information Fig. S5A and Fig. 4I). In addition, there was a considerable increase in F4/80 positive cells in KO → WT mice in comparison to WT → WT mice following DSS treatment, as seen in Fig. 4J and Fig. S5B. Moreover, the levels of proinflammatory cytokines and chemokines mRNA in the mice colon tissues of KO → WT were significantly elevated than that of WT → WT (Fig. 4K). Overall, these findings indicate that the myeloid-specific JOSD2 deletion exacerbates DSS-induced colitis, indicating that JOSD2 in macrophages plays a crucial role in safeguarding against DSS-induced colitis.

### 3.5. *JOSD2 directly interacts with an inflammation-regulating protein IMPDH2*

To explore the molecular mechanism through which JOSD2 exerts its function in IBD, immunoprecipitation experiments and liquid chromatography-tandem mass spectrometry (LC−MS/MS) were performed to qualitatively analyze JOSD2-binding proteins (Fig. 5A). Interestingly, the LC−MS/MS analysis and immunoprecipitation assay showed that JOSD2 could interact with IMPDH2, an important inflammation-regulating protein (Fig. 5B and C). Recent studies have shown that inhibition of IMPDH2 activity produced anti-inflammatory and immunosuppressive effects[28], and IMPDH2 mediates NF-$\kappa$B activation in viral infection and immunity[29]. Therefore, the potential JOSD2−IMPDH2 interaction, which probably regulates NF-$\kappa$B signal and inflammatory response in IBD, aroused our interest. Then, co-immunoprecipitation (Co-IP) and double immunofluorescence staining experiments further confirmed the interaction between JOSD2 and IMPDH2 *via in vitro* co-transfection of JOSD2-Flag and GFP-IMPDH2-HA plasmids (Fig. 5D and E). To further explore the essential domain of IMPDH2 that interacts with JOSD2, a series of GFP-IMPDH2-HA truncated mutants were constructed to identify the key domain in IMPDH2 protein (Fig. 5F). As shown in Fig. 5G, residues 232−514 of IMPDH2 were indispensable for binding to JOSD2, and this domain belonged to the C-terminal catalytic activity of IMPDH2. Finally, the interaction between endogenous JOSD2 and IMPDH2 in mouse primary bone marrow-derived macrophages (BMDMs) was confirmed by Co-IP assay under physiological conditions, and the interaction between JOSD2 and IMPDH2 was further increased when the BMDMs were challenged by lipopolysaccharide (LPS) (Fig. 5H). Additionally, endogenous JOSD2 and IMPDH2 also interacted with each other in the mouse colon tissues (Supporting Information Fig. S6). Collectively, these data confirm the direct interaction between JOSD2 and IMPDH2.

### 3.6. *JOSD2 mediates K63-linked deubiquitination of IMPDH2 at lysine 134*

An *in vitro* investigation was conducted to study the mechanism of action by which JOSD2 affects the activity of IMPDH2. The plasmid encoding GFP-IMPDH2-HA was simultaneously transfected with plasmids encoding Ub-Myc, JOSD2-Flag, or JOSD2-C24A-Flag into HEK293T cells. Fig. 6A demonstrates a significant decrease in the ubiquitination of IMPDH2 when JOSD2 was present. However, when there was a mutation in the active site cysteine 24 (C24A) of JOSD2, the levels of deubiquitination were significantly restored (Fig. 6A). It has been determined that the Cys24 residue in the Josephin domain is essential for the enzymatic function of JOSD2 that deubiquitinates the substrates[30]. Furthermore, JOSD2 exhibited an enhanced capacity to deubiquitinate IMPDH2 dose-dependently in HEK293T cells (Fig. 6B). Deubiquitination assays were performed using WT, K6-, K11, K27, K29, K33, K48-, K63-, and K48R-linked ubiquitin chains to better establish the specific ubiquitin chain type on IMPDH2 that is influenced by JOSD2. The study revealed that JOSD2 effectively eliminated K63-linked ubiquitin chains from IMPDH2, as seen in Fig. 6C and D and Supporting Information Fig. S7A. Furthermore, an investigation was conducted to examine the lysine residues in IMPDH2 that might potentially be linked to the deubiquitination alteration facilitated by JOSD2. Five key lysine sites in IMPDH2 were replaced with arginine to create the K124R, K134R, K349R, K422R, and K489R mutants of IMPDH2. In HEK293T cells, overexpression of JOSD2 effectively counteracted the ubiquitination of IMPDH2 when co-transfected with K124R, K349R, K422R, and K489R mutants (Fig. 6E). However, this reversal did not occur in cells co-transfected with K134R mutants, indicating that K134 in IMPDH2 is essential for JOSD2-mediated deubiquitination. As shown in Supporting Information Fig. S8A, the amino acid K134 is conserved throughout a wide range of taxa, including *Danio rerio* and different mammals. Altogether, these findings demonstrate that JOSD2 cleaves K63-linked polyubiquitin of IMPDH2 at K134.

We next evaluated the binding by co-immunoprecipitation experiments *via in vitro* co-transfection of JOSD2-Flag with GFP-IMPDH2-HA plasmids or GFP-IMPDH2-K134R-HA plasmids in primary mouse peritoneal macrophages (MPMs). As shown in the Supporting Information Fig. S9A, the interaction between JOSD2 and IMPDH2-K134R was decreased in macrophages. Furthermore, compared to the wide-type IMPDH2, the ubiquitination level of IMPDH2-K134R mutant was significantly reduced and JOSD2 failed to further deubiquitinate IMPDH2-K134R mutant, indicating that K134 in IMPDH2 is essential for ubiquitination and JOSD2-mediated deubiquitination (Fig. S9B).

### 3.7. *JOSD2 inhibits the activity of IMPDH2 to suppress downstream NF-κB activation*

The effect of JOSD2 on IMPDH2 activation in colon tissues and macrophages was also investigated. The Western blot analysis revealed that the absence of JOSD2 did not significantly impact the protein abundance of IMPDH2 in the colon tissues, suggesting that JOSD2 may not regulate the protein stability of IMPDH2 (Fig. 7A). The effect of JOSD2 on the enzyme activity of IMPDH2 in co-transfection HEK293T cells was further evaluated. The results showed that JOSD2 overexpression decreased enzyme activity of

treated with LPS (100 ng/mL) for 8 h ($n = 4$). (J) BMDMs were prepared from WT mice. Cells were transfected with GFP-IMPDH2-HA or GFP-IMPDH2-K134R-HA expressing plasmid. Then were treated with LPS (100 ng/mL) for 30 min. Lysates then were probed for activation of downstream NF-$\kappa$B pathway proteins. Total proteins and GAPDH were used as control. Data are presented as mean ± SD. *$P < 0.05$, **$P < 0.01$, and ***$P < 0.001$.

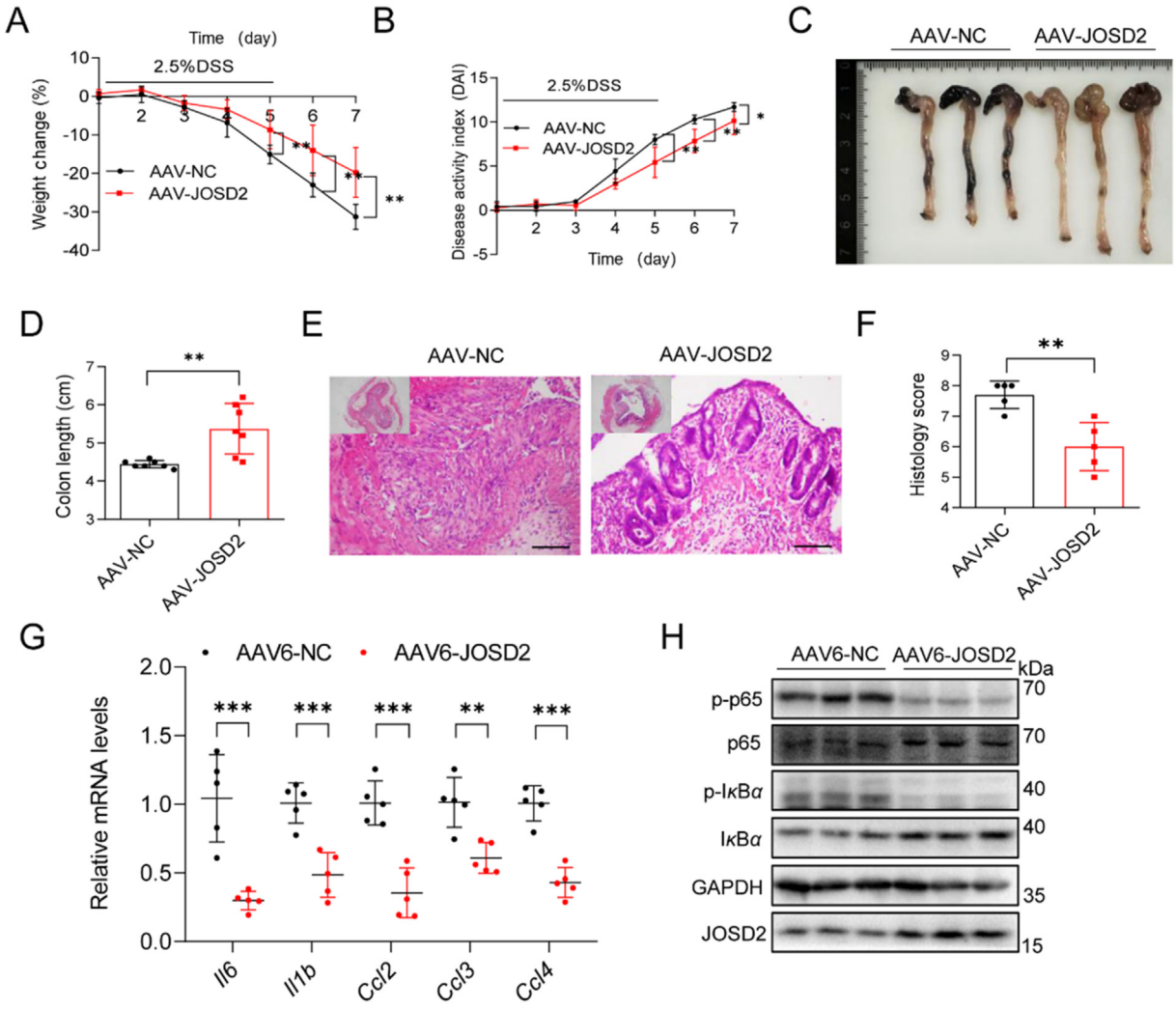


**Figure 8** Increased expression of JOSD2 in macrophages relieves experimental colitis in mice. (A, B) Weight change (A) and DAI (B) for AAV6-NC and AAV6-JOSD2 mice with DSS-induced colitis were assessed daily ($n = 7$). (C, D) Representative images of colons (C) and colon length (D) from the two groups on Day 7 after DSS treatment ($n = 7$). (E, F) Representative images of H&E (E) in distal colon cross-sections from AAV6-NC and AAV6-JOSD2 mice with DSS-induced colitis and semi-quantitative scoring of histopathology (F) ($n = 5$), scale bars = 100 μm. (G) Relative mRNA levels of inflammation-related genes (*Il6*, *Il1b*, *Ccl2*, *Ccl3*, and *Ccl4*) in the colons of mice from the AAV6-NC or AAV6-JOSD2-treated groups ($n = 5$). (H) Representative Western blots analysis of phosphorylated and total p65, and IκBα expression in the colons of AAV6-NC- or AAV6-JOSD2-injected DSS-induced mice. GAPDH served as the loading control ($n = 3$). Data are presented as the mean ± SD. $^*P < 0.05$, $^{**}P < 0.01$, and $^{***}P < 0.001$.

IMPDH2 in cells, but was not able to reduce the protein level of IMPDH2 (Fig. 7B). Lack of JOSD2 resulted in significant inflammatory responses, characterized by increased levels of cytokines and chemokines, in LPS-stimulated JOSD2-KO BMDMs compared to WT BMDMs (Fig. 7C). BMDMs isolated from *Josd2*$^{-/-}$ mice exhibited increased production of IL-6 and IL-1$\beta$ in the cellular supernatants following LPS stimulation compared to macrophages derived from WT mice (Fig. 7D). Western blot assay also showed that JOSD2 was significantly increased in LPS-challenged BMDMs, while the level of IMPDH2 was not changed (Supporting Information Fig. S10A and S10B). A previous study has indicated that IMPDH2 has a role in regulating the NF-κB signal pathway[29]. Thus, primary BMDMs from *Josd2*$^{-/-}$ and WT mice were utilized to assess the activity of NF-κB. According to Fig. 7E, the NF-κB activity level was significantly higher in LPS-treated KO BMDMs than in WT BMDMs. To further examine the effect of JOSD2 on IMPDH2 activation, mycophenolic acid (MPA), an IMPDH2 inhibitor, was used to stimulate BMDMs from KO mice, and then macrophages were stimulated with LPS. As shown in Fig. 7F, NF-κB activity was increased in LPS-challenged BMDMs, while the IMPDH2 inhibitor significantly inhibited the NF-κB activity in BMDMs from KO mice.

To further confirm whether the lysine 134 site was required for IMPDH2 activity and downstream NF-κB activation, IMPDH2 K134R mutant expression was rescued in HEK293T cells by transfection. The result showed that JOSD2 did not affect IMPDH2 K134R enzyme activity (Fig. 7G). IMPDH2 K134R mutant also reversed the expression of *Il6*, *Il1b*, and *Ccl2* mRNA following LPS stimulation (Fig. 7H). Consistently, the IL-6 and IL-1$\beta$ levels in the supernatants of LPS-stimulated macrophages were dramatically decreased in WT BMDM mice by transfection

with an IMPDH2 K134R mutant (Fig. 7I). Similarly, LPS significantly induced p65 and IκBα phosphorylation and IκBα degradation in BMDMs with WT-IMPDH2, but failed in BMDMs with IMPDH2-K134R mutant (Fig. 7J). Overall, these results suggest that IMPDH2 K134R reverses JOSD2-mediated IMPDH2 and NF-κB activities.

### 3.8. *Therapeutic effects of restoring JOSD2 expression against DSS-induced colitis in mice*

In order to investigate the therapeutic potential of JOSD2 in colitis, the adeno-associated virus 6 with macrophage-specific CD68 promoter and JOSD2 plasmid (AAV6-JOSD2) was injected in the mice subjected to DSS-induced colitis to achieve the macrophage-specific overexpression of JOSD2 in mice. The control, AAV6-NC, had enhanced green fluorescent protein (EGFP) overexpression. Fluorescence and real-time quantitative PCR (RT-qPCR; Supporting Information Fig. S11A and S11B) were used to confirm high-efficiency expression. In the DSS-induced colitis model, JOSD2 overexpression significantly reduced body weight loss and the DAI score (Fig. 8A and B). Similarly, compared with the AAV6-NC group, AAV6-mediated JOSD2 overexpression significantly inhibited DSS-induced colon shortening and colon epithelial damage in mice, as seen in Fig. 8C−F. Moreover, AAV6-mediated JOSD2 overexpression markedly reduced the expression of proinflammatory cytokine and chemokine genes compared with the AAV6-NC-injected group (Fig. 8G). The immunoblot analysis further confirmed that the levels of phosphorylated-p65 and phosphorylated-IκBα were markedly decreased in colon tissues in AAV6-mediated JOSD2 overexpression mice (Fig. 8H). In summary, these findings indicate that the use of AAV6 to increase the expression of JOSD2 provides protection against colitis produced by DSS in mice.

### 3.9. *JOSD2 deficiency exacerbates the development of AOM/DSS-induced CRC in mice*

To conduct a comprehensive analysis and investigate the involvement of JOSD2 in the progression of colitis-associated CRC using a well-established animal model produced by AOM/DSS. The Supporting Information Fig. S12A displays the schematic chronology of the experiment with the mice model. The findings indicated that *Josd2*$^{-/-}$ mice exhibited a significant reduction in survival rate upon comparison to WT mice following AOM/DSS therapy (Fig. S12B). Furthermore, *Josd2*$^{-/-}$ mice treated with AOM/DSS exhibited a higher incidence of colon tumors that were larger when compared to their WT littermates (Fig. S12C−S12E). The H&E staining results revealed the presence of high-grade dysplasia in the colons of *Josd2*$^{-/-}$ mice and low-grade dysplasia of adenomas in WT littermates (Fig. S12F). The IHC staining showed a significant increase in Ki67-positive cells after AOM/DSS administration in the colon tissues of *Josd2*$^{-/-}$ mice relative to WT mice (Fig. S12G). Immunoblot analysis was also performed to evaluate the level of JOSD2 in colon tumor tissues. As shown in Fig. S12H, the level of JOSD2 was markedly increased in the colon tumor tissues of WT mice when compared to normal colon tissues. IHC staining for JOSD2 was also performed in the mouse cancer samples, showing a high expression level of JOSD2 in colon cancer tissues from mice with AOM/DSS (Fig. S12I). The findings verified that JOSD2 deficiency exacerbates the development of AOM/DSS-induced CAC.

## 4. Discussion

The present study demonstrated that a DUB, JOSD2, alleviated colitis by deubiquitinating IMPDH2 and inhibiting IMPDH2 activity in macrophages. The present study reveals the underlying mechanism of the JOSD2−IMPDH2/NF-κB proinflammatory signal axis. It shows that JOSD2 binds directly to the C-terminal catalytic domain of IMPDH2 and cleaves the K63-linked polyubiquitin of IMPDH2 at K134. This cleavage inhibits the activity of IMPDH2, suppressing the downstream NF-κB activation and the release of inflammatory cytokines. Phenotypically, JOSD2 knockout significantly exacerbated DSS-induced inflammatory colitis and increased AOM/DSS-induced CRC development in mice, whereas AAV6-mediated JOSD2 overexpression in macrophages exerted therapeutic effects on colitis-affected mice. The available evidence suggests that one possible treatment approach for IBD is to target JOSD2.

It is essential to highlight that abnormal and persistent inflammatory responses have a role in the development of IBD. Various DUBs have been demonstrated to have a role in the development of IBD *by* modifying the functioning of the intestinal barrier and immune responses[10]. An ovarian tumor protease family member called A20 functions as a DUB and inhibits the synthesis of proinflammatory cytokines in macrophages by modulating the NF-κB signaling pathway. Additionally, A20 alleviates the development of colitis produced by DSS in mice[31]. Another investigation further showed that A20 hinders the process of necroptosis in intestinal epithelial cells by eliminating K63-linked polyubiquitin chains from receptor-interacting protein kinase 3[32]. *JOSD2* was initially identified as an oncogene. JOSD2 has been shown to promote cholangiocarcinoma progression by deubiquitinating and stabilizing YAP/TAZ[16]. JOSD2 facilitates the growth of hepatocellular carcinoma by interacting with and impeding the degradation of CTNNB1[17]. In an earlier investigation, it was found that JOSD2 controlled the regulation of intracellular calcium and improved the dysfunction and hypertrophy of the heart caused by Ang II *via* acting on SERCA2a in mice[19]. JOSD2 also blocks nuclear localization of PKM2 by decreasing its K433 acetylation and decreases AML progression[33]. Studies have also shown the importance of the glycolytic enzyme PMK2 in inflammatory diseases, so PKM2 may also be a JOSD2 substrate mediating inflammation, which is worthy of further investigation[34,35]. The present investigation observed elevated expression of JOSD2 in both mouse macrophages following DSS administration and in the intestinal macrophages of individuals with UC and CD. In addition, the absence of *Josd2* in either the entire body or specifically in myeloid cells worsened the colitis generated by DSS, leading to increased damage to epithelial cells, infiltration of inflammatory cells, and tissue death. Furthermore, *Josd2*$^{-/-}$ mice exhibited a more significant number of larger, higher-grade tumors in the colon as compared to the WT littermates in the AOM/DSS model. The data indicate a new role of JOSD2 in the development of both colitis and CRC.

Intestinal homeostasis is a process that requires balancing the host's response to the healthy gut microbiome with the potential for pathogenic stimuli. Disruption of the gut's homeostasis can cause intestinal inflammation, which in turn exacerbates due to immune system malfunction, ultimately resulting in inflammatory bowel disease[36]. A recent investigation has produced a comprehensive map of the specific alterations in gene expression that take place in adaptive immune cells throughout the development of UC. The study also proposes that $CD8^+$ tissue-resident memory T cells may

play a significant role in IBD[37]. The study also found that caspase recruitment domain-containing protein 9 (CARD9) is expressed in neutrophils but not in epithelial or $CD11c^+$ cells. This expression of CARD9 in neutrophils provides protection against DSS-induced colitis[38]. There is also growing evidence that macrophages can serve as a very promising drug target for modulating the intestinal immune system and inflammatory microenvironment, thereby easing the inflammatory response in colitis. Shen et al.[39] and Du et al.[40] showed that both resident and recruited macrophages can be seen in the intestinal space. It is thought that during UC, resident macrophages reduce inflammation, while recruited macrophages produce proinflammatory effector cells[41,42]. The current study has several limitations as well. For instance, KO mice specific to macrophages were not employed. However, the significance of macrophage JOSD2 was corroborated by the *in vitro* cell tests, *in vivo* animal investigations, and bone marrow transplantation protocols utilizing promoter-specific AAV6. Future research on intestinal macrophages in colitis ought to focus on modifying the inflammatory phenotype while preserving the protective tissue-resident subpopulations because there are various intestinal macrophage subsets with considerable heterogeneity and unique functional features[43].

IMPDH is a key rate-limiting enzyme that takes part in the manufacture of *de novo* guanine nucleotide and is widely expressed in immune cells[44]. Humans have two IMPDH isoforms, IMPDH1 and IMPDH2, which share 84% sequence homology at the protein level. However, unlike IMPDH1, IMPDH2 is highly expressed in rapidly proliferating immune cells in multiple inflammation-related diseases, as well as neoplastic cells, and changes in IMPDH2 levels impact the invasion or proliferation of cancer cells[28,45,46]. The two primary domains of IMPDH2 are the tandem cystathionine-$\beta$-synthase (CBS) domains that are evolutionarily conserved and the catalytic domain for substrate interaction. Together, these domains create the Bateman domain[47]. Although not necessary for catalysis, the Bateman domain interacts with the catalytic domain to communicate and has a significant allosteric regulatory influence on IMPDH2 activity. According to recent research, IMPDH2 degradation is mediated by BTBD9, an adapter of the Cullin−RING ligase complex[48]. According to *in vivo* ubiquitination experiments, IMPDH2 was mostly ubiquitinated at K11, K29, and K63 instead of K48[48]. Our study discovered for the first time that JOSD2 combines with the C-terminal catalytic domain of IMPDH2 and then deubiquitinating IMPDH2 to negatively regulate its activity, further influencing the downstream NF-$\kappa$B signal pathway. Additionally, we discovered that JOSD2 regulates IMPDH2 activity through the K134 lysine site. This study also strongly supports the role of IMPDH2 in mediating macrophage inflammation and colitis through NF-$\kappa$B signaling pathway.

In addition, we think that the increase in JOSD2 expression should be a negative feedback in colon tissues of mice with colitis. Under the physiological circumstance, the expression of JOSD2 in macrophages is very low. Under colitis condition, in order to reduce inflammation, macrophages induce high expression of JOSD2, which then deubiquitinates IMPDH2 activity and inhibits IMPDH2−NF-$\kappa$B inflammatory pathway. Therefore, the up-regulation of JOSD2 expression should be pathologically induced, suggesting that gene therapy introducing JOSD2 could serve as a novel therapeutic strategy for colitis treatment. Direct injection of recombinant JOSD2 protein into mouse colon tissue *via* a delivery system of biodegradable targeted materials might be a promising and potential therapeutic strategy for colitis. Of course, it is still unknown how JOSD2 transcription is up-regulated in colitis mouse macrophages. This is a limitation of our work and deserves further study.

## 5. Conclusions

The present work shows that JOSD2 directly interacts with IMPDH2 and, *via* K63-linked deubiquitination, reduces IMPDH2 activity in macrophages. By suppressing the IMPDH2/NF-$\kappa$B signaling pathway, macrophage JOSD2 minimizes colon inflammation and inhibits the development of DSS-induced colitis. According to the present research, JOSD2 targeting may be a potential therapeutic strategy for intestinal inflammatory illnesses such as IBD and CRC.

## Acknowledgments

We graciously thank Professor Fuping You at Peking University for sharing the whole-body *Josd2*$^{-/-}$mice. This study was supported by the National Natural Science Foundation of China (82300589 to Xin Liu, 82004042 to Mincong Huang, and 82370244 to Yi Wang) and the Zhejiang Provincial Key Scientific Project (2021C03041 to Guang Liang, China).

## Author contributions

Xin Liu: Writing − original draft. Yi Fang: Methodology. Mincong Huang: Data curation. Shiliang Tu: Project administration. Boan Zheng: Formal analysis. Hang Yuan: Formal analysis. Peng Yu: Investigation. Mengyao Lan: Methodology. Wu Luo: Validation. Yongqiang Zhou: Methodology. Guorong Chen: Validation. Zhe Shen: Project administration. Yi Wang: Software. Guang Liang: Writing − review & editing.

## Conflicts of interest

The authors have declared that no conflict of interest exists.

## Appendix A. Supporting information

Supporting information to this article can be found online at https://doi.org/10.1016/j.apsb.2024.12.012.

## References

1. Sung H, Ferlay J, Siegel RL, Laversanne M, Soerjomataram I, Jemal A, et al. Global cancer statistics 2020: GLOBOCAN estimates of incidence and mortality worldwide for 36 cancers in 185 countries. *CA Cancer J Clin* 2021;**71**:209−49.
2. Siegel RL, Miller KD, Sauer AG, Fedewa SA, Butterly LF, Anderson JC, et al. Colorectal cancer statistics, 2020. *CA Cancer J Clin* 2020;**70**:145−64.
3. Faye AS, Holmer AK, Axelrad JE. Cancer in inflammatory bowel disease. *Gastroenterol Clin North Am* 2022;**51**:649−66.
4. Parikh K, Antanaviciute A, Fawkner-Corbett D, Jagielowicz M, Aulicino A, Lagerholm C, et al. Colonic epithelial cell diversity in health and inflammatory bowel disease. *Nature* 2019;**567**:49−55.
5. Wallace KL, Zheng LB, Kanazawa Y, Shih DQ. Immunopathology of inflammatory bowel disease. *World J Gastroenterol* 2014;**20**:6−21.
6. Roda G, Ng SC, Kotze PG, Argollo M, Panaccione R, Spinelli A, et al. Crohn's disease. *Nat Rev Dis Primers* 2020;**6**:22.

7. Kobayashi T, Siegmund B, Le Berre C, Wei SC, Ferrante M, Shen B, et al. Ulcerative colitis. *Nat Rev Dis Primers* 2020;**6**:74.
8. Song Y, Yuan M, Xu Y, Xu H. Tackling inflammatory bowel diseases: targeting proinflammatory cytokines and lymphocyte homing. *Pharmaceuticals* 2022;**15**:1080.
9. Kao AT, Cabanlong CV, Padilla K, Xue X. Unveiling ferroptosis as a promising therapeutic avenue for colorectal cancer and colitis treatment. *Acta Pharm Sin B* 2024;**14**:3785−801.
10. Ruan J, Schlüter D, Naumann M, Waisman A, Wang X. Ubiquitin-modifying enzymes as regulators of colitis. *Trends Mol Med* 2022;**28**:304−18.
11. Popovic D, Vucic D, Dikic I. Ubiquitination in disease pathogenesis and treatment. *Nat Med* 2014;**20**:1242−53.
12. Clague MJ, Barsukov I, Coulson JM, Liu H, Rigden DJ, Urbe S. Deubiquitylases from genes to organism. *Physiol Rev* 2013;**93**:1289−315.
13. Bednash JS, Mallampalli RK. Regulation of inflammasomes by ubiquitination. *Cell Mol Immunol* 2016;**13**:722−8.
14. Lei H, Yang L, Xu HZ, Wang ZT, Li XY, Liu M, et al. Ubiquitin-specific protease 47 regulates intestinal inflammation through deubiquitination of TRAF6 in epithelial cells. *Sci China Life Sci* 2022;**65**:1624−35.
15. Wu B, Qiang LH, Zhang Y, Fu YS, Zhao MY, Lei ZH, et al. The deubiquitinase OTUD1 inhibits colonic inflammation by suppressing RIPK1-mediated NE-kappa B signaling. *Cell Mol Immunol* 2022;**19**:276−89.
16. Qian MJ, Yan FJ, Wang WH, Du JM, Yuan T, Wu RL, et al. Deubiquitinase JOSD2 stabilizes YAP/TAZ to promote cholangiocarcinoma progression. *Acta Pharm Sin B* 2021;**11**:4008−19.
17. Huang Y, Zeng JX, Liu T, Xu QY, Song XL, Zeng JH. Deubiquitinating enzyme JOSD2 promotes hepatocellular carcinoma progression through interacting with and inhibiting CTNNB1 degradation. *Cell Biol Int* 2022;**46**:1089−97.
18. Krassikova L, Zhang BX, Nagarajan D, Queiroz AL, Kacal M, Samakidis E, et al. The deubiquitinase JOSD2 is a positive regulator of glucose metabolism. *Cell Death Differ* 2021;**28**:1091−109.
19. Han J, Fang Z, Han B, Ye B, Lin W, Jiang Y, et al. Deubiquitinase JOSD2 improves calcium handling and attenuates cardiac hypertrophy and dysfunction by stabilizing SERCA2a in cardiomyocytes. *Nat Cardiovasc Res* 2023;**2**:764−77.
20. Lin W, Ma C, Su F, Jiang Y, Lai R, Zhang T, et al. Raf kinase inhibitor protein mediates intestinal epithelial cell apoptosis and promotes IBDs in humans and mice. *Gut* 2017;**66**:597−610.
21. Zhang J, Cen L, Zhang XF, Tang CX, Chen YS, Zhang YW, et al. MPST deficiency promotes intestinal epithelial cell apoptosis and aggravates inflammatory bowel disease *via* AKT. *Redox Biol* 2022;**56**:102469.
22. Liu X, Luo W, Chen J, Hu C, Mutsinze RN, Wang X, et al. USP25 deficiency exacerbates acute pancreatitis *via* up-regulating TBK1−NF-$\kappa$B signaling in macrophages. *Cell Mol Gastroenterol Hepatol* 2022;**14**:1103−22.
23. Qian JF, Liang SQ, Wang QY, Xu JC, Luo W, Huang WJ, et al. Isoproterenol induces MD2 activation by $\beta$-AR−cAMP−PKA−ROS signalling axis in cardiomyocytes and macrophages drives inflammatory heart failure. *Acta Pharmacol Sin* 2024;**45**:531−44.
24. Wirtz S, Neufert C, Weigmann B, Neurath MF. Chemically induced mouse models of intestinal inflammation. *Nat Protoc* 2007;**2**:541−6.
25. Dunkern T, Chavan S, Bankar D, Patil A, Kulkarni P, Kharkar PS, et al. Design, synthesis and biological evaluation of novel inosine 5′-monophosphate dehydrogenase (IMPDH) inhibitors. *J Enzyme Inhib Med Chem* 2014;**29**:408−19.
26. Hou Y, Shi GD, Guo YF, Shi JG. Epigenetic modulation of macrophage polarization prevents lumbar disc degeneration. *Aging-Us* 2020;**12**:6558−69.
27. Yao D, Dong M, Dai C, Wu S. Inflammation and inflammatory cytokine contribute to the initiation and development of ulcerative colitis and its associated cancer. *Inflamm Bowel Dis* 2019;**25**:1595−602.
28. Liao LX, Song XM, Wang LC, Lv HN, Chen JF, Liu D, et al. Highly selective inhibition of IMPDH2 provides the basis of antineuroinflammation therapy. *Proc Natl Acad Sci U S A* 2017;**114**:E5986−94.
29. Li TW, Kenney AD, Park JG, Fiches GN, Liu HL, Zhou DW, et al. SARS-CoV-2 Nsp14 protein associates with IMPDH2 and activates NF-$\kappa$B signaling. *Front Immunol* 2022;**13**:1007089.
30. Seki T, Gong LJ, Williams AJ, Sakai N, Todi SV, Paulson HL. JosD1, a membrane-targeted deubiquitinating enzyme, is activated by ubiquitination and regulates membrane dynamics, cell motility, and endocytosis. *J Biol Chem* 2013;**288**:17145−55.
31. Pu T, Liu WZ, Wu YJ, Zhao Y. A20 functions as a negative regulator in macrophage for DSS-induced colitis. *Int Immunopharmacol* 2021;**97**:107804.
32. Zhou MX, He J, Shi YY, Liu XM, Luo SJ, Cheng C, et al. ABIN3 negatively regulates necroptosis-induced intestinal inflammation through recruiting A20 and restricting the ubiquitination of RIPK3 in inflammatory bowel disease. *J Crohns Colitis* 2021;**15**:99−114.
33. Lei H, Yang L, Wang YY, Zou ZH, Liu M, Xu HZ, et al. JOSD2 regulates PKM2 nuclear translocation and reduces acute myeloid leukemia progression. *Exp Hematol Oncol* 2022;**11**:42.
34. Xie M, Yu Y, Kang R, Zhu S, Yang LC, Zeng L, et al. PKM2-dependent glycolysis promotes NLRP3 and AIM2 inflammasome activation. *Nat Commun* 2016;**7**:13280.
35. Shirai T, Nazarewicz RR, Wallis BB, Yanes RE, Watanabe R, Hilhorst M, et al. The glycolytic enzyme PKM2 bridges metabolic and inflammatory dysfunction in coronary artery disease. *J Exp Med* 2016;**213**:337−54.
36. Pan XH, Zhu Q, Pan LL, Sun J. Macrophage immunometabolism in inflammatory bowel diseases: from pathogenesis to therapy. *Pharmacol Ther* 2022;**238**:108176.
37. Boland BS, He ZR, Tsai MS, Olvera JG, Omilusik KD, Duong HG, et al. Heterogeneity and clonal relationships of adaptive immune cells in ulcerative colitis revealed by single-cell analyses. *Sci Immunol* 2020;**5**:eabb4432.
38. Danne C, Michaudel C, Skerniskyte J, Planchais J, Magniez A, Agus A, et al. CARD9 in neutrophils protects from colitis and controls mitochondrial metabolism and cell survival. *Gut* 2023;**72**:1081−92.
39. Sheng JP, Ruedl C, Karjalainen K. Most tissue-resident macrophages except microglia are derived from fetal hematopoietic stem cells. *Immunity* 2015;**43**:382−93.
40. Du J, Zhang JL, Wang L, Wang X, Zhao YX, Lu JY, et al. Selective oxidative protection leads to tissue topological changes orchestrated by macrophage during ulcerative colitis. *Nat Commun* 2023;**14**:3675.
41. Zigmond E, Bernshtein B, Friedlander G, Walker CR, Yona S, Kim KW, et al. Macrophage-restricted interleukin-10 receptor deficiency, but not IL-10 deficiency, causes severe spontaneous colitis. *Immunity* 2014;**40**:720−33.
42. Zigmond E, Varol C, Farache J, Elmaliah E, Satpathy AT, Friedlander G, et al. Ly6C$^{hi}$ monocytes in the inflamed colon give rise to proinflammatory effector cells and migratory antigen-presenting cells. *Immunity* 2012;**37**:1076−90.
43. Ma SJ, Zhang JX, Liu HS, Li S, Wang Q. The role of tissue-resident macrophages in the development and treatment of inflammatory bowel disease. *Front Cell Dev Biol* 2022;**10**:896591.
44. Zimmermann AG, Gu JJ, Laliberte J, Mitchell BS. Inosine-5′-monophosphate dehydrogenase: regulation of expression and role in cellular proliferation and T lymphocyte activation. *Prog Nucleic Acid Res Mol Biol* 1998;**61**:181−209.
45. Zhang Q, Cui KS, Yang XY, He QL, Yu J, Yang L, et al. c-Myc−IMPDH1/2 axis promotes tumourigenesis by regulating GTP metabolic reprogramming. *Clin Transl Med* 2023;**13**:e1164.
46. Kofuji S, Hirayama A, Eberhardt AO, Kawaguchi R, Sugiura Y, Sampetrean O, et al. IMP dehydrogenase-2 drives aberrant nucleolar activity and promotes tumorigenesis in glioblastoma. *Nat Cell Biol* 2019;**21**:1003−14.
47. Hedstrom L. IMP Dehydrogenase: structure, mechanism, and inhibition. *Chem Rev* 2009;**109**:2903−28.
48. Gao ZF, Wang AZ, Zhao YX, Zhang XX, Yuan XS, Li NN, et al. Integrative proteome and ubiquitinome analyses reveal the substrates of BTBD9 and its underlying mechanism in sleep regulation. *Acs Omega* 2022;**7**:11839−52.